In presenting this dissertation as partial fulfillment of the requirements for an advanced degree from the Georgia Institute of Technology, I agree that the Library of the Institute shall make it available for inspection and circulation in accordance with its regulations governing materials of this type.

I agree that permission to copy from, or to publish from, this dissertation may be granted by the professor under whose direction it was written, or, in his absence, by the Dean of the Graduate Division when such copying or publication is solely for scholarly purposes and does not involve potential financial gain.

It is understood that any copying from, or publication of, this dissertation which involves potential financial gain will not be allowed without written permission.

Olin Stewart Lord

CONTRIBUTION OF INDIVIDUAL WELDS TO THE ULTIMATE STRENGTH OF A GROUP OF FILLET WELDS

A THESIS

Presented to

The Faculty of the Graduate Division

by

Olin Stewart Lord

In Partial Fulfillment

of the Requirements for the Degree

Master of Science in Civil Engineering

Georgia Institute of Technology

June, 1963

5 A
12 T

CONTRIBUTION OF INDIVIDUAL WELDS TO THE ULTIMATE STRENGTH OF A GROUP OF FILLET WELDS

Approved:

[redacted]

Date approved by Chairman: 5 September 196

ACKNOWLEDGMENTS

The writer wishes to thank all whose advice and generosity contributed to the successful completion of this thesis. I am deeply indebted to Dr. F. W. Schutz, Jr. for stimulating interest in connections in general and welded connections in particular, and for guidance and encouragement throughout this investigation.

To Dr. A. B. Caseman and Dr. C. E. Stoneking go thanks for their comments and suggestions incorporated in this thesis.

A portion of the steel plate used in this investigation was donated by the Bethlehem Steel Company. Appreciation is also extended to the J. J. Finnigan Company, Inc. for their excellent cooperation in the fabrication of the test specimens.

TABLE OF CONTENTS

	Page
ACKNOWLEDGMENTS	ii
LIST OF TABLES	iv
LIST OF ILLUSTRATIONS	v
NOMENCLATURE	vi
SUMMARY	ix
Chapter	
I. INTRODUCTION	1
II. THEORETICAL DEVELOPMENT	4
III. DESCRIPTION OF TESTS	29
IV. DISCUSSION OF RESULTS	37
V. COMPARISON WITH STANDARD AMERICAN PRACTICE	52
VI. CONCLUSIONS AND SUGGESTIONS FOR FURTHER STUDY	55
VII. SUMMARY OF TENTATIVE RECOMMENDATIONS FOR DESIGN OF FILLET	57
APPENDIX	
A. TABLES	60
B. FIGURES	71
BIBLIOGRAPHY	84

LIST OF TABLES

Table		Page
1.	Actual Dimensions of Test Specimens	61
2.	Tensile Coupon Results for Parent Steel	64
3.	Tensile Coupon Results for Deposited Weld Material	64
4.	Test Results and Analysis for Longitudinal Welds with Concentric Loading	65
5.	Test Results and Analysis for Transverse Welds with Concentric Loading	65
6.	Test Results and Analysis for a Combination of Two Longitudinal Welds and One Transverse Weld with Concentric Loading	66
7.	Test Results and Analysis for Two Longitudinal Welds with Eccentric Loading	66
8.	Test Results and Analysis for One Transverse Weld with Eccentric Loading	67
9.	Test Results and Analysis for a Combination of Two Longitudinal Welds and One Transverse Weld with Eccentric Loading	67
10.	Comparison of Theoretical Loads for Concentrically Loaded Joints Using a Standard Method and the Proposed Method	69
11.	Comparison of Theoretical Loads for Eccentrically Loaded Joints Using a Standard Method and the Proposed Method	69

LIST OF ILLUSTRATIONS

Figure		Page
1a.	Direction and Location of Stresses on the Weldment	72
1b.	General Dimensions of Test Specimens	72
1c.	Comparison of Theoretical Ultimate Loads	73
2.	Test Specimens Loaded in Tension	74
3.	Test Specimens Loaded in Shear and Torsional Moment	75
4.	Test Specimens Loaded in Shear, Torsional Moment and Tension	75
5.	Typical Coupon Layout on Steel Plate	76
6.	Typical Testing Arrangement	77
7.	Instrumentation of Tensile Specimens	78
8.	Test Specimen Before Loading	79
9.	Test Specimen After Loading	80
10.	Instrumentation of Specimens Loaded in Shear and Torsional Moment	81
11.	Instrumentation of Specimens Loaded in Shear, Torsional Moment and Tension	81
12.	Load Vs Average Elongation of Weld Material Curves for Specimens IIbmA, IIbmB and IIbmR	82
13.	Load Vs Average Elongation of Weld Material Curves for Specimens IamR, 1, 2 and 3	82
14.	Load Vs Average Elongation of Weld Material Curves for Specimens IIasA, 1, 2 and 3	83
15.	Load Vs Average Elongation of Weld Material Curves for Specimens IIIcmA, 1, 2 and 3	83

NOMENCLATURE

Longitudinal - Axis parallel to main axis of test specimen. Axis is referred to as x axis. All angles are measured from this axis. A longitudinal weldment bears no relation as to the direction of loading.

Transverse - Axis perpendicular to main axis of test specimen. Axis is referred to as y axis. A transverse weldment bears no relation as to the direction of loading.

σ_c - Comparison stress obtained by use of interaction formula.

σ_ω - Ultimate tensile stress of deposited weld material.

σ_s - Stress level in steel plates.

σ_y - Yield stress of steel plates.

$\sigma_\perp$ - A tensile or compression stress on the throat area acting perpendicular to the throat section in a fillet.

$\tau_\perp$ - A shear stress on the throat area acting in a direction transverse to the length of the fillet and lying in the plane of the throat section.

$\tau_{\parallel}$ - A shear stress on the throat area acting along the length of the fillet and lying in the plane of the throat section.

N - A tensile or compressive stress on the throat area acting in a direction perpendicular to the fillet weld and in the plane of the connection.

λ - Stress factor.

P - Externally applied load.

ℓ_1 - Length of transverse weld.

a_1 - Throat depth of transverse weld.

ℓ_2 - Length of longitudinal weld.

a_2 - Throat depth of longitudinal weld.

h - Transverse width of parent steel strip that is connected to larger steel strip by fillet welds to firm a joint.

P_x - Externally applied load parallel to x axis.

P_y - Externally applied load parallel to y axis.

e - Eccentricity of load: The distance measured from the centroid of the weld group to line of action of externally applied load, P.

θ - Angle between externally applied load and the x axis.

M_T - Torsional moment.

$M'_{z_{11}}$ - Moment capacity of two longitudinal welds due to stresses parallel to the axis of the welds if the transverse stresses are ignored.

M'_N - Moment capacity of a longitudinal weld due to the transverse stresses if the longitudinal stresses are ignored.

M_{LL} - Proportion of total moment carried by longitudinal weld due to stress parallel to axis of longitudinal weld.

M_{LT} - Proportion of total moment carried by longitudinal weld due to stress transverse to axis of longitudinal weld.

M'_L - Moment capacity of two longitudinal welds due to stresses parallel to the axis of the longitudinal welds if the transverse stresses are ignored and there is one transverse weld present in the joint.

M'_B - Moment capacity of one transverse weld due to transverse stresses if the longitudinal stresses are ignored.

M_{TT} - Proportion of total moment carried by transverse weld due to stress transverse to axis of transverse weld.

P'_L - Shear load resisted by longitudinal welds.

P'_B - Shear load resisted by transverse weld.

P_L - Proportion of total shear load resisted by longitudinal welds.

P_B - Proportion of total shear load resisted by transverse weld.

$$Q = \frac{M'_{z_{11}}}{M_{z_{11}} + 2M'_N(l_2/l_1)}$$

$$K = \frac{M'_L}{M'_L + M'_B}$$

$$J = \frac{P'_L}{P'_L + P'_B}$$

R - Ratio of actual test load to theoretical load.

SUMMARY

This investigation had as its objective the determination of the contribution of individual welds to the ultimate strength of a group of fillet welds. An interaction theory on fillet weld groups proposed for use in design by the International Institute of Welding was used to design the test specimens. The experimental results were used to prove or disprove the validity of this interaction theory.

Test specimens were fabricated from steel plates and tested with concentric and eccentric loads. The specimens conformed to a definite program which consisted of series of specimens. Each series was designed so that relations between certain variables could be determined. Pertinent variables were ratios of lengths of the weldments, ratios of throat depths of the weldments and the stress level in the connected steel.

It was found from the test results that the general interaction theory as proposed is valid but that the proposed constant for use in the interaction formula is in serious error. An adjustment of this constant as dictated by the test results was made. The theoretical ultimate loads were then found to be in close agreement with all the actual ultimate loads obtained from the test specimens.

Using the corrected interaction formula design formulas for various fillet weld groups were derived. These groups consisted of "U" shaped joints, joints with side welds only and joints with end welds only. The formulas derived for these joints are limited to loads in the plane of the weld group but the loads may be concentric or eccentric to the axis

of the weld group.

Conclusions drawn from this investigation indicate:

1. Varying the ratio of areas of the weldments is a more significant parameter for investigation of a connection than the ratio of lengths or the ratio of throat depths of the weldments.

2. The stress level in the connected plates has a very significant effect upon the strength of a connection.

3. Ductility is of major importance in obtaining high efficiency in a connection.

4. The basic interaction theory on fillet weld groups proposed by the International Institute of Welding is valid but the proposed constants for use in the interaction formula should be modified.

CHAPTER I

INTRODUCTION

Welded connections usually consist of a group of welds rather than a single weld and the welds are usually subjected to one or more types of loading simultaneously. Contribution of individual welds to the ultimate strength of the group depends upon their orientation to the other welds and also their orientation to the force system acting upon the group in addition to other variables. These conditions present a formidable, if not impossible, task with regard to obtaining solutions by elastic theory for many cases. But the situation readily lends itself to plastic theory so long as the material being connected is ductile and the weld material itself is ductile.

For welded connections in ductile material the following assumptions can be made only when the ultimate strength is being considered and the parent material and the welds are stressed beyond the elastic limit.

1. Local stress peaks due to the configuration of the joint are not considered.

2. Uniform distribution of stresses throughout the length of weld is assumed.

3. Residual stresses are not considered.

These assumptions are true for the static strength of a connection if the materials are sufficiently ductile.

By use of plastic theory and an ultimate strength concept this

investigation was carried out on concentrically and eccentrically loaded fillet welded connections with the following objectives:

1. Determine effect of varying the ratio of lengths of transverse and longitudinal welds.

2. Determine effect of varying the ratio of throat depths of transverse and longitudinal welds.

3. Determine effect of varying the stress level in the connected plates.

4. Investigate significance of the ductility of the deposited weld metal.

5. Investigate the validity of an interaction theory on fillet weld groups proposed for design by the International Institute of Welding and modify these if necessary.

Because of eccentricities and discontinuities inherent in fillet-welded connections the actual distribution of stresses and the interaction of the group of welds is extremely complex.

The experimental investigation was carried out by testing series of steel plate (ASTM Designation-A36) connections with each series designed so as to fully exploit the interaction of one set of variables. One major variable was changed with each series and other variables were varied within a series.

Practically all research conducted in recent years toward establishing formulas for calculating strength of welded connections submitted to static loads has been conducted under Commission XV of the International Institute of Welding. The Netherland delegation to this commission has been the major contributor of information.

Based on results of tests conducted under Commission XV the proposed interaction formula[1]* for use in determining a comparison stress is is:

$$\sigma_c = \sqrt{\sigma_\perp^2 + \lambda(\tau_\perp^2 + \tau_{//}^2)} \qquad (1)$$

Values determined from this equation are compared to tensile test rupture stresses for the deposited weld metal. Information obtained from tests in the Netherlands[1] indicate that the value for λ should be 1.8, and this value has been tentatively adopted by Commission XV of the IIW. This formula will be used in the analysis of test results from the experimental investigation in an attempt to prove or disprove its validity.

* Numbers in parenthesis are references found in the Bibliography.

CHAPTER II

THEORETICAL DEVELOPMENT

The formula, $\sigma_c = \sqrt{\sigma_\perp^2 + \lambda(\tau_\perp^2 + \tau_{\parallel}^2)}$, is applicable only to joints in which the different welds lie in the same plane and are subjected to forces and moments lying in that plane. Only this type of connection will be investigated. Furthermore, for simplicity only connections with symmetrical weld groups composed of transverse and longitudinal welds will be considered. Joints will be classified according to the type of forces acting upon the weld groups, that is, concentric longitudinal, concentric transverse and torsional moment in the weld plane. Figures 1a and 1b indicate the physical significance of symbols used in this chapter.

Theoretical equations that might be used for design purposes will be developed in this chapter. The equations will be based on the formula, $\sigma_c = \sqrt{\sigma_\perp^2 + 1.8(\tau_\perp^2 + \tau_{\parallel}^2)}$, and they will apply to joints as described above. Equations will be derived for concentrically and eccentrically loaded joints with two longitudinal welds, one transverse weld and also for a combination of two longitudinal welds and one transverse weld. Later these equations will be used in examing test results.

Concentric Loading

A joint loaded with a concentric force can develop tensile, compression and shear stresses depending upon the orientation of the welds to the direction of the force. Using the interaction formula, welds with particular orientation will be analyzed.

A. Concentric Longitudinal Load on Longitudinal Welds

The only stress considered will be a shear stress (τ_{11}) parallel to the direction of load and the axis of the fillet weld. This stress is assumed to be uniformly distributed along the weld. Therefore:

$$\tau_{11} = \frac{P}{\Sigma h_2 a_2} \qquad (2)$$

Using equation 1 and $\lambda = 1.8$

$$\sigma_c = \sqrt{1.8(\tau_{11})^2} = 1.34\,\tau_{11}$$

where σ_c is to be compared to an established ultimate tensile stress.

Then:

$$\tau_{11} = \frac{\sigma_c}{1.34} = 0.75\,\sigma_c = \frac{P}{\Sigma h_2 a_2} \qquad (3)$$

so when a safety factor is included for a practical application:

$$\tau_{11} = \frac{P}{\Sigma h_2 a_2} = 0.75\,\sigma_a \qquad (3a)$$

where σ_a is the allowable tensile stress.

B. Concentric Longitudinal Load on Transverse Welds

With this case there will be normal and shear stresses acting perpendicular to the axis of the fillet weld. Assuming the fillet cross section forms an isosceles right triangle so that the throat is at forty five degrees the combined stress will be:

$$N = \frac{P}{\Sigma l_1 a_1}$$

then the stress on the throat is:

$$\sigma_\perp = N \cos 45^\circ = \frac{P}{\Sigma l_1 a_1} \cos 45^\circ = \frac{P}{\Sigma l_1 a_1} \frac{1}{\sqrt{2}} \qquad (4)$$

$$\tau_\perp = N \sin 45^\circ = \frac{P}{\Sigma l_1 a_1} \sin 45^\circ = \frac{P}{\Sigma l_1 a_1} \frac{1}{\sqrt{2}} \qquad (5)$$

therefore, $\sigma_\perp = \tau_\perp$.

Using equation 1 and $\lambda = 1.8$:

$$\sigma_c = \sqrt{\sigma_\perp^2 + 1.8\,\tau_\perp^2} = \sigma_\perp \sqrt{2.8} = \tau_\perp \sqrt{2.8}$$

$$\sigma_c = \sqrt{2.8}\ \frac{P}{\sqrt{2}\,\Sigma l_1 a_1} = \sqrt{1.4}\ \frac{P}{\Sigma l_1 a_1}$$

where σ_c is to be compared to an established ultimate tensile stress of the deposited weld metal.

Then:

$$\frac{P}{\Sigma l_i a_i} = 0.85\,\sigma_c \qquad (6)$$

so when a safety factor is included for a practical application:

$$\frac{P}{\Sigma l_i a_i} = 0.85\,\sigma_a \qquad (6a)$$

where σ_a is the allowable tensile stress.

C. Concentric Longitudinal Load on Group of Transverse and Longitudinal Welds

In this case there is an interaction between the welds such that the ultimate strength of the joint is not the sum of the strengths of the separate welds. Ductility of the materials involved is a major parameter in determining the ultimate strength of the joint. However, geometry of the joint also influences the relative effect of the ductility. So, for analysis purposes, joints have been classified according to the ratio of the length of the transverse weld to the length of the longitudinal weld.

Pending completion of research now under way the following methods are provisionally recommended by the International Institute of Welding.(1)

These provisional recommendations will be used by the writer strictly on a comparative basis. Their validity will be discussed at length in the discussion on results of this experimental study.

Class I - Long Longitudinal Weld: $\ell_2 > 1.5\ell_1$. For joints where the longitudinal weld length is greater than 1.5 times the transverse weld length no load should be attributed to the transverse weld. Deformation in the longitudinal weld is such that rupture of the transverse weld will occur before full utilization of the load carrying capacity of the longitudinal weld. Therefore, the formula for only longitudinal welds should be used in this case.

$$\frac{P}{\Sigma \ell_2 a_2} = 0.75\ \sigma_a \qquad (7)$$

Class II - Longitudinal and Transverse Welds Approximately Equal: $0.5\ell_1 < \ell_2 \leq 1.5\ell_1$. When the lengths of the two types of welds are close in magnitude and the joint is "U" shaped (i.e. only one transverse weld present) the ultimate strength of the joint will be approximately equal to the sum of the strength of the longitudinal weld and one-third the strength derived for a transverse weld alone. This empirical formula is based on previous test conducted by the International Institute of Welding.

$$P = \left(0.75(\Sigma \ell_2 a_2) + \tfrac{1}{3} \times 0.85(\Sigma \ell_1 a_1)\right)\sigma_a$$

$$P = \left(0.75\left(\Sigma \ell_2 a_2\right) + 0.28\left(\Sigma \ell_1 a_1\right)\right)\sigma_a \qquad (8)$$

Class III - Short Longitudinal Weld: $\ell_2 \leq 0.5\,\ell_1$. If the longitudinal welds are much shorter than the transverse welds, the transverse welds will assume practically all the load. Because the greater rigidity of the transverse welds restricts deformation in the longitudinal welds the contribution of the longitudinal welds is very limited. As dictated by previous test data the strength is reduced to one-third that derived for a longitudinal weld alone plus the strength of the transverse weld.

$$P = \left(\tfrac{1}{3} \times 0.75\left(\Sigma \ell_2 a_2\right) + 0.85\left(\Sigma \ell_1 a_1\right)\right)\sigma_a$$

$$P = \left(0.25\left(\Sigma \ell_2 a_2\right) + 0.85\left(\Sigma \ell_1 a_1\right)\right)\sigma_a \qquad (9)$$

Based on these empirical relationships the predicted ultimate loads of a series of connections having variable l_2/l_1 ratios are shown in Figure 1c. For purposes of the illustration a total length of weld of 12.0 inches and a throat depth of 0.25 inches were used. The weld metal was assumed to have an ultimate tensile strength of 70,000 psi.

Eccentric Loading

A joint with eccentric loading develops torsional moment and shear forces in the connecting material. To handle these and to transform them into stresses ($\sigma_\perp$, $\tau_\perp$ and $\tau_{//}$) for use in the interaction formula some simplifying assumptions must be made.

Two common methods for handling a torsional problem such as this are "polar moment" method and the "two force" method. The "polar moment" method based on assumed elastic behavior is more general but the "two force" method is more straight forward and the calculations are less cumbersome. So that the interaction formula can be worked out involving only previously used terms and remain relatively simple for comparison purposes the "two force" method will be used here. Recent tests conducted in Germany[1] show both methods to be conservative and both methods yield equivalent results when the ratio of l_2 to l_1 is approximately 0.5 to approximately 2.0.

Use of the "two force" method involves the following assumptions:

1) Uniform distribution of stresses along the throat surface of a weld.

2) Center of rotation is located at the center of gravity of the weld group.

3) $0.5 \leqslant l_2/l_1 \leqslant 2.0$.

In order to derive equations for a concentrated load at any angle and location (but limited to the plane of the weld group) reference axes must be established. The longitudinal axes of the joint will be designated as the X axis and all angles will be referenced to this axis. The axis will pass through the center of gravity of the weld group.

A. Two Longitudinal Welds

For convenience the eccentric load is transposed into an equivalent centroidal load plus a torsional moment. The centroidal load is broken into components. Thus the shear forces will be Px and Py and the torsion moment will equal P x e.

The torsion moment can be represented by two forces of magnitude F. These forces will form a couple with the moment arm approximately equal to h plus a_2.

$$M_T = P_x e = F(h + a_2) \qquad (10)$$

This ignores the presence of transverse stresses in the weld.

By use of equation 2 we find that the couple produces longitudinal shear stress in the welds as follows:

$$\tau_{11} = \frac{2F}{\Sigma l_2 a_2} = \frac{2Pe}{(\Sigma l_2 a_2) + (h + a_2)} \qquad (11)$$

The stresses produced by the loads P_x and P_y are determined by use of equations 2, 4 and 5 respectively.

$$\sigma_\perp = \tau_\perp = \frac{P_y}{\sqrt{2}\,\Sigma l_2 a_2} \qquad (12)$$

$$\tau_{11} = \frac{P_x}{\Sigma h_2 a_2} \qquad (13)$$

then from equation 1: $\sigma_c = \sqrt{\sigma_\perp^2 + 1.8(\tau_\perp^2 + \tau_{11}^2)}$

$$\sigma_c = \sqrt{2.8\left(\frac{P_y}{\sqrt{2}\,\Sigma h_2 a_2}\right)^2 + 1.8\left(\frac{P_x}{\Sigma h_2 a_2} + \frac{2Pe}{(\Sigma h_2 a_2)(h+a_2)}\right)^2} \qquad (14)$$

where $P_y = P\sin\theta$, $P_x = P\cos\theta$

$$\sigma_c = \frac{P}{\Sigma h_2 a_2}\sqrt{1.4\sin^2\theta + 1.8\left(\cos\theta + \frac{2e}{h+a_2}\right)^2} \qquad (14a)$$

σ_c is the stress at the end of the weld.

The preceding derivation ignores any additional stress on the weld material due to bending or rotation of each individual weld about its centroid. In order to evaluate the error resulting from this simplification the following derivation is presented. The contributions from the

two types of moment resistance outlined above will be prorated and added together to obtain the total moment carrying capacity for this type joint.

As presented above (equation 11) the stresses parallel to the longitudinal welds form a couple which has the following moment capacity if the transverse stresses are ignored.

$$\sigma_c = \sqrt{1.8\,\tau_{11}} = \sqrt{1.8\left(\frac{2Pe}{(\Sigma \ell_2 a_2)(h+a_2)}\right)^2}$$

$$M'_{\tau_{11}} = Pe = \frac{1}{2\sqrt{1.8}}(\Sigma \ell_2 a_2)(h+a_2)\sigma_c \qquad (15)$$

$$M'_{\tau_{11}} = 0.37(\Sigma \ell_2 a_2)(h+a_2)\sigma_c \qquad (15a)$$

As the transverse stress varies linearly over the length of the weld for bending or rotation of the individual longitudinal weld about its centroidal axis the torsional formula ($\sigma = \frac{Mc}{J}$) can be used to evaluate the moment capacity.

Therefore:

$$N = \frac{M'_N c}{J} = \frac{M'_N}{\frac{a_2 \ell_2^3}{12}} \quad \frac{\ell_2}{2} = \frac{6M'_N}{a_2 \ell_2^2}$$

This deviates somewhat from the ultimate strength concept but in the absence of experimental evidence revealing more about the movement of the neutral axis as the ultimate load is approached this conservative approach will be used. The axis shifts because a fillet weld is much stronger and more rigid in compression and also due to plastification of the weld material as the stresses approach and exceed the elastic limit of the material. The shifting of the axis and plastification of the weld metal assures that this approach is conservative.

Then:

$$\sigma_\perp = \tau_\perp = \frac{1}{\sqrt{2}} N = \frac{6M'_N}{\sqrt{2}\, a_2 \ell_2^2} \qquad (16)$$

For $2M'_N = P \times e$

$$\sigma_\perp = \tau_\perp = \frac{6Pe}{\sqrt{2}\,(\Sigma a_2 \ell_2)\ell_2} \qquad (16a)$$

From the above equation the torsional moment resisted by the two longitudinal welds is as follows:

$$\sigma_c = \sqrt{2.8\left(\frac{6Pe}{\sqrt{2}\,(\Sigma a_2 \ell_2)\ell_2}\right)^2}$$

$$2M'_N = \frac{1}{6\sqrt{1.4}}(\Sigma a_2 \ell_2)\ell_2 \sigma_c = 0.14(\Sigma a_2 \ell_2)\ell_2 \sigma_c \qquad (17)$$

Because of compatibility of failure strains it may not be possible to develop the moment, $2M'_N$, fully. Multiplication of $2M'_N$ by ℓ_2/ℓ_1 will adjust the moment relation such that strain compatibility is recognized. The total torsional moment, $M_T = Pe$, can now be proportioned between $M'_{z_{11}}$ and $2M'_N$.

$$M_{LL} = \left(\frac{M'_{z_{11}}}{M'_{z_{11}} + 2M'_N(\ell_2/\ell_1)}\right) M_T \qquad (18)$$

where $$\frac{M'_{z_{11}}}{M'_{z_{11}} + 2M'_N(\ell_2/\ell_1)} = \frac{0.37(4+a_2)}{0.37(4+a_2)+0.14\ell_2(\ell_2/\ell_1)} = Q \qquad (19)$$

$$M_{LT} = \left(\frac{2M'_N(\ell_2/\ell_1)}{M'_{z_{11}} + 2M'_N(\ell_2/\ell_1)}\right) M_T \qquad (20)$$

where $$\frac{2M'_N(k_2/k_1)}{M'_{z_{11}} + 2M'_N(k_2/k_1)} = \frac{0.14k_2(k_2/k_1)}{0.37(h+a_2)+0.14k_2(k_2/k_1)} = 1-Q \qquad (21)$$

Therefore the stresses due to torsional moment are:

$$z_{11} = \frac{2QPe}{(\Sigma k_2 a_2)(h+a_2)} \qquad (22)$$

$$\sigma_\perp = z_\perp = \frac{6(1-Q)Pe}{\sqrt{2}(\Sigma a_2 k_2^2)} \qquad (23)$$

The stresses produced by the loads P_x and P_y are determined by use of equations 2, 4 and 5 respectively.

$$\sigma_\perp = z_\perp = \frac{P_y}{\sqrt{2}(\Sigma k_2 a_2)} \qquad (24)$$

$$z_{11} = \frac{P_x}{\Sigma k_2 a_2} \qquad (25)$$

then from equation 1: $\sigma_c = \sqrt{\sigma_1^2 + 1.8(\tau_t^2 + \tau_{11}^2)}$

$$\sigma_c = \sqrt{2.8\left(\frac{P_y}{\sqrt{2}(\Sigma h_2 a_2)} + \frac{6(1-Q)Pe}{\sqrt{2}(\Sigma a_2 h_2^2)}\right)^2 + 1.8\left(\frac{P_x}{\Sigma h_2 a_2} + \frac{2QPe}{(\Sigma h_2 a_2)(h+a_2)}\right)^2} \qquad (26)$$

where Py = Psinθ, PX = P cosθ, equation 12 reduces to:

$$\sigma_c = \frac{P}{\Sigma h_2 a_2}\sqrt{1.4\left(\sin\theta + \frac{6(1-Q)e}{l_2}\right)^2 + 1.8\left(\cos\theta + \frac{2Qe}{h+a_2}\right)^2} \qquad (26a)$$

The magnitude of the error induced by ignoring transverse stress on a weld group caused by torsional moment can now be determined. Upper and lower bound limits for the ratio of l_2 to l_1 ($0.5 \leq l_2/l_1 \leq 2.0$) as stated in the assumptions at the beginning of this chapter will be used for the evaluation of the error range.

Assume $l_2/l_1 = 0.5$ and $a_2 = 0.166$ in.

then

$$Q = \frac{0.37(h+a_2)}{0.37(h+a_2) + 0.14 h_2 (h_2/l_1)} = 0.92$$

For lower bound conditions assume $\theta = 90°$, e = 8 in., l_2 = 1.5 in., a_2 = 0.166 in. Let S equal Eq. 26a / Eq. 14a.

Then:

$$S = \frac{\frac{P}{\Sigma a_2 l_2}\sqrt{1.4\left(1+\frac{0.08\times 6\times 8}{1.5}\right)^2 + 1.8\left(\frac{2\times 0.92\times 8}{3+0.166}\right)^2}}{\frac{P}{\Sigma a_2 l_2}\sqrt{1.4+1.8\left(\frac{2\times 8}{3+0.166}\right)^2}} = 1.09$$

Assume l_2/l_1 = 2.0 and a_2 = 0.166 in.

Then:

$$Q = \frac{0.37(4+a_2)}{0.37(4+a_2)+0.14 l_2 (l_2/l_1)} = 0.41$$

For upper bound conditions assume $\theta = 90°$, e = 8 in., l_2 = 3 in., a_2 = 0.166 in.

$$S = \frac{\frac{P}{\Sigma a_2 l_2}\sqrt{1.4\left(1+\frac{0.59\times 6\times 8}{3.0}\right)^2 + 1.8\left(\frac{2\times 0.41\times 8}{1.5+0.166}\right)^2}}{\frac{P}{\Sigma a_2 l_2}\sqrt{1.4+1.8\left(\frac{2\times 8}{1.5+0.166}\right)^2}} = 1.04$$

Errors of 9 per cent and 4 per cent for the lower and upper boundaries respectively are of insignificant magnitude. Therefore the transverse stress caused by torsional moment can be ignored.

B. Single Transverse Weld

The stress distribution for this weld is identical to that assumed in the previous section for torsion of the weld about its centroidal axis. Therefore, from the previous section (equation 16a) the stresses due to bending will be as follows:

$$\sigma_{\perp} = \tau_{\perp} = \frac{6Pe}{\sqrt{2}\,\Sigma a_i \ell_i^2} \qquad (27)$$

Assuming a uniform distribution of the shear stresses due to concentrically applied loads, equations 2, 4 and 5 can be used to determine the magnitude of the stresses due to P_x and P_y.

$$\tau_{\parallel} = P_y / \Sigma a_i \ell_i \qquad (28)$$

$$\sigma_{\perp} = \tau_{\perp} = P_x / \sqrt{2}\,\Sigma a_i \ell_i \qquad (29)$$

So from equation 1: $$\sigma_c = \sqrt{2.8\left(\frac{6Pe}{\sqrt{2}(\Sigma a_1 l_1^2)} + \frac{P_x}{\sqrt{2}(\Sigma a_1 l_1)}\right)^2 + 1.8\left(\frac{P_y}{\Sigma a_1 l_1}\right)^2} \quad (30)$$

Where $P_y = P\sin\theta$, $P_x = P\cos\theta$

$$\sigma_c = \frac{P}{\Sigma a_1 l_1}\sqrt{1.4\left(\frac{6e}{h} + \cos\theta\right)^2 + 1.8\sin^2\theta} \quad (30a)$$

σ_c is the stress at the end of the weld.

C. Combination of Two Longitudinal Welds and a Single Transverse Weld

From equations 11 and 1 the torsional moment resisted by the longitudinal welds produces a stress as follows:

$$\sigma_c = \sqrt{1.8\,\tau_{11}^2} = \sqrt{1.8\left(\frac{2M_t}{(\Sigma l_2 a_2)(h + a_2)}\right)^2} \quad (31)$$

From this equation the moment capacity of the longitudinal welds is found to be:

$$M_L' = \frac{1}{2\sqrt{1.8}} (\Sigma \ell_2 a_2)(h + a_2)\sigma_c = 0.37(\Sigma \ell_2 a_2)(h + a_2)\sigma_c \qquad (32)$$

Equation 32 ignores the presence of transverse stresses on the longitudinal welds.

From equation 27 the torsional moment resisted by the transverse weld is as follows:

$$\sigma_c = \sqrt{\sigma_L^2 + 1.8\tau_L^2} = \sqrt{2.8\left(\frac{6M_B'}{\sqrt{2}(\Sigma a_1 \ell_1^2)}\right)^2} \qquad (33)$$

$$M_B' = \frac{1}{6\sqrt{1.4}} (\Sigma a_1 \ell_1)\ell_1 \sigma_c = 0.14(\Sigma a_1 \ell_1)\ell_1 \sigma_c \qquad (34)$$

The torsion moment, $M_T = Pe$, can now be proportioned between M_L' and M_B'.

$$M_{LL} = \left(\frac{M_L'}{M_L' + M_B'}\right) M_T \qquad (35)$$

where $$\frac{M'_L}{M'_L + M'_B} = \frac{0.37(\Sigma \ell_2 a_2)(h + a_2)}{0.37(\Sigma \ell_2 a_2)(h + a_2) + 0.14(\Sigma a_1 \ell_1)\ell_1} = K \qquad (36)$$

$$M_{TT} = \frac{M'_B}{M'_L + M'_B} \qquad (37)$$

where $$\frac{M'_B}{M'_L + M'_B} = \frac{0.14(\Sigma a_1 \ell_1)\ell_1}{0.37(\Sigma \ell_2 a_2)(h + a_2) + 0.14(\Sigma a_1 \ell_1)\ell_1} = 1 - K \qquad (38)$$

Substitute the value of M_{LL} into equation 31 to find the stress on the longitudinal welds due to the total torsional moment:

$$\tau_{11} = \frac{2KPe}{(\Sigma \ell_2 a_2)(h + a_2)} \qquad (39)$$

Substitute the value of M'_{TT} into equation 33 to find the stress on the transverse weld due to the total torsional moment:

$$\sigma_\perp = \tau_\perp = \frac{6Pe(1-K)}{\sqrt{2}(\Sigma a_1 \ell_1)\ell_1} \qquad (40)$$

The distribution of the shear stresses due to concentric loads is handled in a like manner. From equation 2, 4 and 5 the shear resisted by the longitudinal welds is as follows:

$$\sigma_c = \sqrt{2.8\left(\frac{P_y}{\sqrt{2}(\Sigma \ell_2 a_2}\right)^2 + 1.8\left(\frac{P_x}{\Sigma \ell_2 a_2}\right)^2} \qquad (41)$$

$$= \sqrt{2.8\left(\frac{P\sin\theta}{\sqrt{2}(\Sigma \ell_2 a_2)}\right)^2 + 1.8\left(\frac{P\cos\theta}{\Sigma \ell_2 a_2}\right)^2}$$

$$= \frac{P}{\Sigma \ell_2 a_2}\sqrt{1.4\sin^2\theta + 1.8\cos^2\theta}$$

therefore: $$P_L' = \frac{(\Sigma \ell_2 a_2)\sigma_c}{\sqrt{1.4\sin^2\theta + 1.8\cos^2\theta}} \qquad (42)$$

From equation 2, 4 and 5 the shear resisted by the transverse welds, following the procedures used above, is as follows:

$$\sigma_c = \sqrt{2.8\left(\frac{P_x}{\sqrt{2}(\Sigma \ell_1 a_1}\right)^2 + 1.8\left(\frac{P_y}{\Sigma \ell_1 a_1}\right)^2} \qquad (43)$$

$$\sigma_c = \sqrt{2.8\left(\frac{P\cos\theta}{\sqrt{2}(\Sigma \ell_1 a_1}\right)^2 + 1.8\left(\frac{P\sin\theta}{\Sigma \ell_1 a_1}\right)^2}$$

$$= \frac{P}{\Sigma \ell_1 a_1}\sqrt{1.4\cos^2\theta + 1.8\sin^2\theta}$$

$$P_B' = \frac{(\Sigma \ell_1 a_1)\sigma_c}{\sqrt{1.4\cos^2\theta + 1.8\sin^2\theta}} \qquad (44)$$

The load P can now be proportioned between P_L' and P_B' .

$$P_L = \left(\frac{P_L'}{P_L' + P_B'}\right)P \qquad (45)$$

where $$\frac{P_L'}{P_L' + P_B'} = \frac{\dfrac{\Sigma \ell_2 a_2}{\sqrt{1.4\sin^2\theta + 1.8\cos^2\theta}}}{\dfrac{\Sigma \ell_2 a_2}{\sqrt{1.4\sin^2\theta + 1.8\cos^2\theta}} + \dfrac{\Sigma \ell_1 a_1}{\sqrt{1.4\cos^2\theta + 1.8\sin^2\theta}}} = J \qquad (46)$$

$$P_B = \left(\frac{P'_B}{P'_L + P'_B} \right) P \tag{47}$$

where $$\frac{P'_B}{P'_L + P'_B} = 1 - J \tag{48}$$

Substitute values of P_L and P_B into equation 2, 4 and 5.

For effect of concentric loads on longitudinal welds:

$$\sigma_\perp = \tau_\perp = \frac{J P_y}{\sqrt{2}\,(\Sigma l_2 a_2)} \tag{49}$$

$$\tau_{\parallel} = \frac{J P_x}{\Sigma l_2 a_2} \tag{50}$$

For effect of concentric loads on transverse welds:

$$\sigma_\perp = \tau_\perp = \frac{(1-J)\, P_x}{\sqrt{2}\,(\Sigma a_1 l_1)} \tag{51}$$

$$\tau_{\parallel} = \frac{(1-J)\, P_y}{\Sigma a_1 l_1} \tag{52}$$

Now, the final equations for the combination joint will be the interaction values for the summation of the stresses in the longitudinal welds and the summation of the stresses in the transverse weld. The interaction value for the longitudinal weld will be calculated by substituting the values from equations 39, 49 and 50 into equation 1. Results from equations 40, 51 and 52 will be used to determine the interaction value for the transverse weld.

$$\sigma_c \text{ (longitudinal welds)} = \sqrt{2.8\left(\frac{JP_y}{\sqrt{2}\,\Sigma h_2 a_2}\right)^2 + 1.8\left(\frac{JP_x}{\Sigma h_2 a_2} + \frac{2KPe}{(\Sigma h_2 a_2)(h+a_2)}\right)^2} \quad (53)$$

$$= \frac{P}{\Sigma h_2 a_2}\sqrt{1.4J^2\sin^2\theta + 1.8\left(J\cos\theta + \frac{2Ke}{h+a_2}\right)^2}$$

$$\sigma_c \text{ (transverse weld)} = \sqrt{2.8\left(\frac{(1-J)P_x}{\sqrt{2}\,\Sigma h_1 a_1} + \frac{(1-K)6Pe}{\sqrt{2}\,(\Sigma h_1 a_1)h}\right)^2 + 1.8\left(\frac{(1-J)P_y}{\Sigma h_1 a_1}\right)^2} \quad (54)$$

$$= \frac{P}{\Sigma h_1 a_1}\sqrt{1.4\left((1-J)\cos\theta + \frac{6(1-K)e}{h}\right)^2 + 1.8(1-J)^2\sin^2\theta}$$

Where σ_c is the stress at the ends of the welds.

In the derivation of equation 14a the effect of the transverse stresses on moment carrying capacity of the longitudinal welds was ignored. The error resulting from this has been demonstrated to be small.

But for the joints with one transverse weld the bending stress could not be ignored because this was the only means of carrying the torsional moment. Now, in equation 54 bending stresses present in the transverse weld are considered and the bending stresses present in the longitudinal welds are again ignored. Since the "U" shaped connection has moment capacity due to the longitudinal stress in the longitudinal weld it is possible to ignore the effect of transverse stresses on the transverse weld. This would be accomplished by assigning a K value of 1.0 in equation 53 and 54 as follows:

$$\sigma_{\text{(longitudinal welds)}} = \frac{P}{\Sigma l_2 a_2}\sqrt{1.4J^2\sin^2\theta + 1.8\left(J\cos\theta + \frac{2e}{h+a_2}\right)^2} \qquad (55)$$

$$\sigma_{\text{(transverse weld)}} = \frac{P}{\Sigma l_1 a_1}\sqrt{1.4(1-J)^2\cos^2\theta + 1.8(1-J)^2\sin^2\theta} \qquad (56)$$

The following is a comparison to determine the error involved using this simplified assumption. Boundary conditions will be assumed.

Assume: $\Sigma l_1 a_1 = \Sigma l_2 a_2$, $\theta = 90°$; $h = 3$ in., $a = 0.166$ in., $J = 0.6$, $K = 0.7$, $e = 8$ in.

$$\sigma_{(55)} = \frac{P}{\Sigma l_2 a_2}\sqrt{1.4(0.6)^2 + 1.8\left(\frac{2\times 8}{3+0.166}\right)^2} = 6.77\,\frac{P}{\Sigma l_2 a_2}$$

$$\sigma_{(56)} = \frac{P}{\Sigma l_1 a_1}\sqrt{1.8(0.4)^2} = 0.54\,\frac{P}{\Sigma l_1 a_1}$$

$$\sigma_{(53)} = \frac{P}{\Sigma l_2 a_2}\sqrt{1.4(0.6)^2 + 1.8\left(\frac{1.4 \times 8}{3 + 0.166}\right)^2} = 4.80\,\frac{P}{\Sigma l_2 a_2}$$

$$\sigma_{(54)} = \frac{P}{\Sigma l_1 a_1}\sqrt{1.4\left(\frac{6 \times 0.3 \times 8}{3}\right)^2 + 1.8(0.4)^2} = 5.70\,\frac{P}{\Sigma l_1 a_1}$$

For the case where all bending is ignored equation 55 controls. For the case where bending in the transverse weld is considered equation 54 controls.

$$\frac{\sigma_{(55)}}{\sigma_{(54)}} = \frac{P/\Sigma l_2 a_2 \times 6.77}{P/\Sigma l_1 a_1 \times 5.70} = 1.19$$

As this is for a boundary condition an error of 19 per cent induced by ignoring bending in the transverse weld is insignificant. Therefore it would be justifiable to simply use equation 55 to predict P_{ult} for this type of joint.

CHAPTER III

DESCRIPTION OF TEST

General

In order to fully explore the variables outlined in Chapter I it was decided that this program should be divided into seven series of tests. Series I, II and III were designed to be loaded concentrically in tension (Figure 2). Series IV and V were designed to be loaded eccentrically in shear and torsional moment (Figure 3). Series VI and VII were designed to be loaded eccentrically in shear, torsional moment and tension (Figure 4). The dimensions and geometric configuration of the specimens can be seen in the figures referred to above.

The Roman Numerals were designated as a code for the ratio of the longitudinal and transverse weld lengths. Each series was further broken down into an a, b and c code to designate the ratio of the longitudinal and transverse weld throat thicknesses. Code letters s, m and h were then added to designate the thickness of the strips as small, medium and large. Then A, B and R were added to indicate if the electrode used was acid, basic or rutile type. Finally, the series were further divided into four categories according to the weld pattern used. These four weld patterns were: (1) a complete "U" shaped weld pattern (2) two longitudinal welds (3) a transverse weld and (4) two longitudinal welds with larger throat dimensions than the previous specimen. A typical series of specimens would be identified as IamR, IamR1, IamR2 and

IamR3. All specimens fabricated for this program, with the code designation and actual dimensions are tabulated in Table 1.

Test Specimens

In order to eliminate as many undesirable variables or by-products of fabrication as possible particular care was taken in planning the fabrication of the test specimens. Steel plate classified as American Society for Testing Material Designation A-36[2] was selected because of its superior welding characteristics. Plate stock was used so that the components of the test specimens could be cut from the interior of the plates thus reducing the effect of residual stresses induced in the steel during the rolling process. To insure as much uniformity in the steel as possible all plates of equal thickness were taken from the same heat. This means the plates of equal thickness had approximately the same chemical and physical properties.

The components of the test specimens were numbered for control purposes and these numbers were scribed onto the surface of the steel plates. A typical lay out is shown in Figure 5. The components were flame cut by an automatic torch. Heat effects from the cutting were small and it was assumed that they were virtually eliminated by milling off the heat affected zone on those edges which were to be welded. Also, during assembly of the specimens care was taken to insure that the welded ends of the components were from the interior of the parent plates and not from a free edge.

Electrodes

In order to obtain some insight as to the effect of a particular

electrode upon the strength of a joint it was decided to use three types. Electrodes can be classified to fall into one of three broad classifications. The classifications are acid, basic and rutile. One electrode was selected from each of these classifications. The American Welding Society specifications for the electrodes selected are listed below.

Rutile: E-7014 (AWS), Iron Powder (approximately 30 per cent) AC or DC

As Welded:	Tensile strength	72 to 80 ksi
	Yield point	60 to 70 ksi
	Elongation	22-30 per cent
	Impact	119 ft. lbs.

Basic: E-7018 (AWS), Low Hydrogen, Iron Powder (approximately 25 per cent) AC or DC

As Welded:	Tensile strength	70 to 80 ksi
	Yield point	60 to 70 ksi
	Elongation	22-30 per cent
	Impact	119 ft. lbs.

Acid: E-6027 (AWS), Mineral, Iron Powder (approximately 50 per cent) AC or DC

As Welded:	Tensile strength	62 to 72 ksi
	Yield point	50 to 64 ksi
	Elongation	25-30 per cent
	Impact	60 ft. lbs.

Determination of Physical Properties

As indicated on the typical pattern layout shown in Figure 5 a strip was provided to be used for tensile coupons adjacent to one edge

of every component of the test specimens. These strips, indicated by the numbers on Figure 5 were milled into standard eight inch gage length tensile coupons and tested according to ASTM specifications.(3) The average data from the coupons associated with a particular series of test specimens is reported in Table 2.

Standard two inch gage length tensile coupons for obtaining properties of the deposited weld material were fabricated, machined and tested according to American Welding Society specifications.(4) Five coupons from each electrode type used in fabricating the test specimens were tested and the averages of the test results are reported in Table 3.

The properties reported for the rutile and acid type electrodes are representative of their performance, but the basic type electrode should have exhibited a greater ductility than that shown in Table 3. Welding of the tensile coupons was done six weeks after welding of the test specimens and during this time the electrodes were stored in a heated cabinet along with many other type electrodes. Temperature in the storage cabinet was high enough for other electrodes but as the basic type was a low hydrogen electrode and its coating has an acute affinity for moisture the temperature should have been higher for this electrode. From this moist coating resulted a high porosity weld metal in the tensile coupons. This had little or no effect on the ultimate tensile strength but severely hampered the ductility. The per cent elongation is reported as 13 per cent but it should have been a minimum of 22 per cent according to the American Welding Society specifications.(4)

From the load-deformation curves for the test specimens welded with the basic type electrode it is obvious that the minimum value of

22 per cent elongation was surpassed. This indicates the dry electrodes had sufficient ductility to meet specifications.

Fabrication

The specimens were fabricated in a local boiler shop by a certified welder. Detailed dimensions (Table 1) and the control number of each component to be used in the make up of each specimen were supplied to the welder. Also, the type of electrode was specified. The commercial brand, required diameter of electrodes, amperage to be used and fabrication procedure were left to the choice and discretion of the welder.

Measurements

All dimensions of the components of the specimens were carefully measured with a machinist micrometer to the nearest thousandth of an inch. Length of the fillet welds were measured to the nearest hundredth of an inch with a graduated scale. Leg length and throat depth were measured with a micrometer dial gage to the nearest five thousandths of an inch.

The throat area was determined by plotting to a large scale on graph paper the measured leg lengths and connecting these two points with a straight line to form a triangle. A line was then erected perpendicular to the hypothenuse and extended through the vertex of the triangle. The measured length of this line multiplied by the measured length of the weld was recorded as the area of the weld. The throat depth measured at forty five degrees by the micrometer dial gage was also plotted as a check to insure that the inscribed triangle was always inside the fillet weld.

In practically all fillets the horizontal leg was slightly longer than the vertical leg. This meant the inscribed throat depth was at some angle slightly greater than forty five degrees measured from the horizontal. This is compatible with the observed rupture planes formed in the test specimens after they were loaded. The rupture plane in the welds was in practically all cases between forty five and sixty degrees measured from the horizontal.

Testing

The specimens were allowed to cure in a dry room at a normal temperature for a period of at least fifteen days after fabrication. The purpose of this waiting period was to allow sufficient time for trapped gases to escape from the deposited weld metal. The initially high hydrogen content which would have caused a more brittle behavior was avoided.

Loading of all the specimens was accomplished in a 45,000 lb. capacity Riehle Mechanical Testing Machine (see Figure 6). A constant strain rate of 0.025 inches per minute was used.

The specimens tested in tension were clamped in the loading heads of the testing machine by wedge shaped jaws and pulled until rupture of the welds occurred. Loading was stopped at constant increments in load, and after the system stablized readings of the elongation to the nearest ten thousandth of an inch were recorded. Elongation of each specimen were determined by a symmetrical arrangement of six micrometer dial gages (Figure 7). Reference points for measurements were as shown in Figure 8 and Figure 9. From this arrangement the total separation of the pull pieces and the elongation of the connecting strips could be measured.

The difference in these two measurements was taken as the average strain in the deposited weld material.

The specimens tested under torsional moment and shear were simply supported at the ends and loaded by a point at mid-span. The testing arrangement and instrumentation was as shown in Figure 10. Rotation within the welded joint was measured by micrometer dial gages.

The specimens tested under torsional moment, shear and tension were pin connected to pull brackets clamped in the loading heads of the testing machine. The testing arrangement and instrumentation was as shown in Figure 11. Rotation within the welded joint and separation of the two pinned ends was measured by micrometer dial gages.

Summary

All tests were considered satisfactory. The specimens exhibited uniformity throughout the testing program. No brittle failures in the steel plates were encountered. Specimens loaded in tension with only the transverse welds failed suddenly with a rapid decrease in load and there was always a loud report at the instant of failure. All specimens with only the longitudinal welds reached an ultimate load after which the load gradually decreased as a progressive shear plane developed in the weldment. This shear plane always originated at the corners of the strip and progressed inward toward the end of the pull pieces. This was caused by bending in the strip which tended to raise the end of the strips and induced a triaxial strain in the weldment. The bending in the strips was produced by the internal moment that was built up during loading from the eccentric loads on the strips.

Specimens with both transverse and longitudinal welds failed in different manners depending upon the ratio of the weld areas. The transverse weld failed first in the specimens loaded in tension and depending upon the relative ratio of area of the longitudinal weld to the transverse weld the failure was either sudden or gradual. All specimens loaded eccentrically reached an ultimate load and then the load decreased gradually as a progressive shear plane developed in the weld metal.

In no case was there ever an appreciable increase in load above the load which caused initial failure of the transverse weld even though considerable more strain had to be applied before failure of the longitudinal welds occurred.

CHAPTER IV

DISCUSSION OF RESULTS

This discussion will be broken down into sections where each section will be concerned with only one particular type joint and loading condition.

Longitudinal Welds with Concentric Loading

These joints were loaded in tension and all such joints are listed in Table 1 as Ixxx2 and 3, IIxxx2 and 3 and IIIxxx2 and 3. All pertinent physical properties are listed. The theoretical ultimate loads calculated from equation 3 using an average ultimate stress for the weld material and also using the actual ultimate stress for the particular type weld material, determined from tensile coupon tests (see Table 3) plus the test results are tabulated in Table 4. The ratio of actual to theoretical ultimate load is shown to aid in evaluating the proposed theory.

From an examination of these ratios it appears that equation 3 is within reason. There is some scatter in the ratios but not enough to implant any doubt that equation 3 will produce adequate predictions for the ultimate load. The largest scatter is for the specimens whose joints contain the longer weldments and or the thicker weldments.

However, there is enough scatter to justify some adjustment to the factor λ. Equation 3 is slightly conservative. An analysis of the test data is shown in Table 4. Only the ultimate test load and the area

of weld material is considered. The relative lengths, throat depth and stress level of the parent steel will be used later to explain scatter of the results.

In Table 4 the load factor was determined by dividing the ultimate stress in the weld material of the joint by some allowable ultimate stress. The allowable stress used was determined by testing tensile coupons from deposited weld material from the electrodes used in fabrication (see Table 3). One factor was calculated by using the ultimate tensile stress for the electrode used to weld the particular joint and another factor was calculated by using an average of the ultimate tensile stresses for the three types of electrodes used.

The numerical average of all the load factors calculated was 0.83. If individual load factors that are of the highest and lowest magnitude are eliminated the average is then approximately 0.8. A load factor of 0.8 agrees well with the test results and the specimens whose test results deviate more than six per cent from a load factor of 0.8 will be discussed in the following paragraphs.

IamR3

The rutile type electrode which has a relatively low ductility and penetration power was used for this specimen. A long, heavy weld coupled with weld material of low ductility tends to produce stress peaks. The stress will not be distributed uniformly along the weld, therefore the average ultimate stress attained will be relatively low.

IbhA2 and 3

The acid type electrode which has high ductility plus deep penetration capabilities was used for these specimens. Even though the weld was

relatively long the measured throat depth was small and with a highly ductile weld material a uniform stress distribution was possible. In addition to possessing high ductility this particular electrode (E-6027) has high penetrating power. This means the effective throat depth is much greater than the measured depth. For smaller measured depths the relative influence of this deep penetration is much greater than for deeper measured throat depths. This fact accounts for the difference between all number 2 and 3 specimens welded with any electrode and has a particular effect on the specimens welded with the E-6027 electrode (referred to in this report as the acid type electrode.) Therefore, high ductility plus deep penetration produced an apparently high average ultimate stress for these specimens.

IcsB2 and 3

The basic type electrode which has medium ductility and penetrating power was used for these specimens. The amount of weld material was large enough to develop a stress level which surpassed the elastic limit of the parent steel. This produced a large deformation in the parent steel and in combination with the ductility of the weld material it was possible to attain a uniform stress level. The relatively shallow measured throat depths in this specimen received contribution from the fully activated penetrated material thus producing a high ultimate stress level.

IIchR3, IIIbsR2 and 3

The rutile type electrode which had relatively low ductility was used for these specimens. The throat depth was relatively large. Thus, a large throat area coupled with low ductility tends to produce stress peaks. This causes a lower average ultimate stress to be attained.

IIIcmA2

The acid type electrode which has high ductility and penetration was used for this specimen. The measured throat depth was small. Therefore, these factors combine to allow a uniform stress distribution and to produce an apparently high ultimate stress level.

All other specimens produce load factors that are in good agreement with the average of 0.8. The slight deviation of each specimen from the average can be attributed to some combination of relative lengths and throat depths and the type electrode used. But the common denominator for all these variables is ductility. If the weld material and parent material are ductile such that a plastic region is formed to allow redistribution of the stresses then the theoretical equation with a load factor of 0.8 predicts the ultimate load of this type connection with sufficient accuracy. Thus, equation 3 should be:

$$P = 0.8(\Sigma t_2 a_2)\sigma_c \qquad (57)$$

Transverse Welds with Concentric Loading

These joints were loaded in tension perpendicular to the axis of the weld. All such joints are listed in Table 1 as Ixxxl, IIxxxl and IIIxxxl. All pertinent physical properties are listed in this table. The theoretical ultimate loads calculated from equation 6 using an average ultimate stress for the weld material and also using the actual ultimate stress for the particular type weld material determined from tensile coupon test (see Table 3) plus the test results are tabulated in Table 5.

The ratio of actual to theoretical ultimate load is shown to aid in evaluating the proposed theory.

Upon examination of the ratios of actual to theoretical ultimate load it appears that equation 6 is in serious error. There is much as a ± 17 per cent deviation from a numerical average of 1.23 for the load factors. This range will be explained later but even the lowest load factor calculated is 21 per cent higher than the theoretical load factor of 0.85 proposed in equation 6. The test data indicates that the transverse weld has considerably greater load carrying capacity than suggested by the proposed theory.

By elimination of the load factors highest and lowest in magnitude and by deductive reasoning it was found that a load factor of 1.2 would be the most logical value to use. The deviation of the calculated load factors from this selected factor can be explained using the variables discussed at length in the previous section. A brief explanation of the behavior of each specimen follows.

IamR1, IIchR1

Ructile electrode, relatively low ductility, results in low ultimate stress.

IamA1, IIasA1

Acid electrode, highly ductile and penetrating, small measured throat depth, results in high ultimate stress.

IcsB1

Basic electrode, medium ductility, large throat depth, results in low ultimate stress.

IIbmBl

Basic electrode, medium ductility, medium throat depth, results in average ultimate stress.

IIIbmBl

Basic electrode, medium ductility, small throat depth, results in high ultimate stress.

IIIbsRl

Ructile electrode, low ductility but high stress level in parent steel medium throat depth, results in average ultimate stress.

IIIcmAl

Acid electrode, high ductility, high stress level in parent steel, large throat depth, results in average ultimate stress.

Again, as in the longitudinal welds, the common denominator for all the variables is ductility. If the physical dimensions of the weld material is limited such that full benefit from its ductility and/or benefit from the ductility of the parent steel is received by producing a high stress level in the steel the theoretical equation 6 with a load factor of 1.2 predicts the ultimate load of this type connection with sufficient accuracy. Thus, equation 6 should be:

$$P = 1.2(\Sigma \ell_i a_i)\sigma_c \qquad (58)$$

Combination of Longitudinal and Transverse Welds with Concentric Loading

These joints were loaded in tension and all such joints are listed in Table 1 as Ixxx, IIxxx and IIIxxx. All pertinent physical properties

are listed. The theoretical ultimate loads calculated from the appropriate equation (equation 7, 8 or 9, which ever fits the geometry of the particular joint in question) using an average ultimate stress for the weld material and also using the actual ultimate stress for the particular type weld material determined from tensile coupon tests (see Table 3) plus the test results are tabulated in Table 6. The ratio of actual to theoretical ultimate load is shown to aid in evaluating the proposed theory. The test results for the previous two sections indicated a need for adjustment of the proposed load factors. As the theory for this section was based upon the theory for the two previous sections a serious disagreement between actual test results and theory should be expected.

In lieu of doggedly following the empirical rules governing geometry of a connection outlined in Chapter II a different procedure for analysis of test results was attempted. The ratios of longitudinal and transverse weld lengths and throat depths was ignored. Only the relative importance of the transverse and longitudinal weld areas was recognized. These areas, multiplied by the load factors arrived at in the two previous sections, were simply added for all specimens. The adjusted areas were then multiplied by an average ultimate tensile stress for the weld material and by the ultimate tensile stress for the particular type weld material. Results from this operation and the ratios of theoretical to actual ultimate load are shown in Table 6.

Using the ultimate tensile stress for the particular type electrode for a specimen the results in Table 6 show excellent agreement between theoretical and actual loads when the stress level in the parent steel exceeded the yield stress of the steel. Maximum errors appear to be no

worse than three per cent on the unconservative side when this condition is realized. However, when the yield stress of the steel is not exceeded the errors are six per cent or greater on the unconservative side. These facts again emphasize the importance of ductility. Upon exceeding the yield stress a plastic region is formed thus allowing a distribution of stresses through the weld.

In order to compensate for this error and receive full efficiency from the connection the welds should be designed such that the theoretical ultimate load is sufficient to produce stresses in excess of the yield stress of the parent steel. Thus, the equation for a "U" shaped joint will be:

$$P = \left(1.2\Sigma l_1 a_1 + 0.8\Sigma l_2 a_2\right)\sigma_c \qquad (59)$$

Two Longitudinal Welds with Eccentric Loading

Specimens listed in Table 1 as IV2 and V2 were loaded under shear and moment. Specimens listed as VI2 and VII2 were loaded under shear, moment and tension. The test results, theoretical ultimate load and ratios of these two loads are also shown in Table 7.

The theoretical load, according to equation 14a, for all specimens is conservative with the degree of conservatism being consistent. As there were only a limited number of specimens loaded eccentrically the relative importance, if any, of many variables cannot be determined. However, following the same general line of reasoning outlined in the sections on concentric loads the following theory will alter that outlined

in Chapter II.

The load factors derived from test results of the tensile specimens should replace the stress factors used in the development of the theory in Chapter II. The basic International Institute of Welding equation (1) will be changed to the following.

For parallel stresses only:

$$\sigma = \sqrt{\lambda \tau_{11}^2} = \sqrt{\lambda \left(\frac{P}{\Sigma \ell a}\right)^2} = \sqrt{\lambda}\, \frac{P}{\Sigma \ell a}$$

$$P = \frac{1}{\sqrt{\lambda}} (\Sigma \ell a)\sigma = 0.8\,(\Sigma \ell a)\sigma$$

$$\lambda = \left(\frac{1}{0.8}\right)^2 = 1.56$$

For perpendicular stresses only:

$$\sigma = \sqrt{\gamma(\sigma_\perp^2 + \tau_\perp^2)} = \sqrt{2\gamma}\, \frac{P}{\sqrt{2}(\Sigma \ell a)}$$

$$P = \frac{1}{\sqrt{\gamma}} (\Sigma \ell a)\sigma = 1.2\,(\Sigma \ell a)\sigma$$

$$\gamma = \left(\frac{1}{1.2}\right)^2 = 0.69$$

Therefore: $$\sigma = \sqrt{0.69(\sigma_I^2 + \tau_I^2) + 1.56\,\tau_{II}^2} \qquad (60)$$

With these stress factors and using equations 11, 12 and 13, equation 14a will change to the following equation for longitudinal welds only.

$$\sigma_c = \frac{P}{\Sigma h_2 a_2}\sqrt{0.35\sin^2\theta + 1.56\left(\cos\theta + \frac{2e}{h+a_2}\right)^2} \qquad (61)$$

The theoretical load calculated from the International Institute of Welding formula (14a) and also formula (61) as altered by test results is listed in Table 7 along with the ratio of theoretical to actual ultimate load. Using the adjusted formula there appears to be a safety factor of about 1.2 against ultimate load. This can be attributed to the fact that part of the welds in the joint are in compression. As the welds are much stronger and more rigid in compression the neutral axis shifts, thus allowing more weld area for the tension region. With only a limited number of tests, further refinements to equation (61) could not be justified. On the basis of the tests that were conducted this equation predicts the ultimate load for this type of joint and loading condition with sufficient accuracy.

One Transverse Weld with Eccentric Loading

Specimens listed in Table 1 as IV1 and V1 were loaded under shear and moment. Specimens listed as VI1 and VII2 were loaded under shear, moment and tension. The test results, theoretical ultimate load and ratios of these two loads are also shown in Table 8.

The theoretical load for all specimens is very conservative with the degree of conservatism being consistent. As in previous sections the theory proposed in Chapter II will be altered by the load factors derived from test results of the tensile specimens with only transverse welds.

Using the stress factors from equation 60 and equations 27, 28 and 29 equation 30 will change to the following equation for transverse welds only.

$$\sigma_c = \frac{P}{\Sigma a_i} \sqrt{0.35\left(\frac{6e}{h} + \cos\theta\right)^2 + 1.56\sin^2\theta} \qquad (62)$$

The theoretical load calculated from the International Institute of Welding formula (30) and also from formula (62) as altered by test results is listed in Table 8 along with the ratio of theoretical to actual ultimate load. With the adjusted formula the safety factor appears to be approximately 1.1 against ultimate load. Again a portion of the weld was in compression but as the joints with the transverse weld had only one weld the magnitude of the shifting of the neutral axis was very small in comparison with that of the longitudinal welds. This allowed very little increase in the area of weld material subject to tension.

The supposedly conservative approach of using the torsion formula ($\sigma = \frac{Mc}{J}$) in the development of the theory in Chapter II is actually very accurate in predicting the ultimate load for joints of this type loaded eccentrically. The torsion formula gives the stress only in the outer fibers up to the yield stress but when the stress in the outer fibers of the weld reach yield in tension they begin to tear before the load is increased an appreciable amount. This is because of the short range between the magnitudes of the yield and ultimate stresses for weld material.

When the tearing begins the neutral axis shifts, thus allowing new area for tension. But, as the weld material is stronger in compression the forces balance and the load carried by the joint remains at a constant magnitude for an amount of rotation depending upon the ductility of the materials involved. This load never rises an appreciable amount above the magnitude of the load at the instant the weld material began to tear.

Combination of One Transverse Weld and Two Longitudinal Welds with Eccentric Loading

Specimens listed in Table 1 as IV and V were loaded under shear and moment. Specimens listed as VI and VII were loaded under shear, moment and tension. The test results, theoretical ultimate load and ratios of these two loads are shown in Table 9.

Again the theoretical load is very conservative with some scatter in the accuracy of the predicted loads. From results stated in the two previous sections this was to be expected.

In order to dispose of the cumbersome techniques proposed in

Chapter II involving the prorating of the forces, etc., a simple combination of equations 61 and 62 derived in the two previous sections from test results is proposed as follows.

$$\sigma_c = \frac{(Eq.\ 61)(Eq.\ 62)}{Eq.\ 61 + Eq.\ 62} \qquad (63)$$

The theoretical ultimate load using the relation described above along with its ratio to the actual ultimate load is listed in Table 9. With the adjusted stress factors and the above relation the adjusted equation gives a safety factor of approximately 1.3 against ultimate load.

Due to the limited amount of test data for eccentrically loaded specimens any further modification of the adjusted equations proposed in the last three sections would not be justified. The theory proposed in these sections will predict the ultimate load for the joints that are within the limits of this theory with sufficient accuracy.

Elongation of the Weld Metal

Curves of load versus elongation of weld metal are shown in Figure 12 thru 15. These are typical curves taken from the test data for specimens tested in this investigation.

Three curves are shown in Figure 12. Each curve is for a particular electrode and also, each curve is the average of three curves from

three test specimens welded with the same electrode. As all nine specimens were fabricated from steel plates from one heat the parent material for all specimens had approximately equal properties (i.e., ductility, yield stress, etc.). Therefore, the difference in the curves is due to variance in the ductility of the three electrodes.

The importance of ductility is clearly evident in this figure. Specimens welded with the rutile electrode ruptured before plastification of the weld material was reached. Thus, all three specimens failed to reach the theoretical ultimate load. Specimens welded with the acid and basic electrodes exhibit a definite plastification of the weld material and all six specimens failed very close to the theoretical ultimate load. Yield stress in the steel plates was exceeded for these six specimens. This aided greatly in the plastification of the weld material. However, in Figure 14 and 15 plastification of the weld material is observed for several specimens where the yield stress of the steel plates was not exceeded. This indicates that if the weld material is sufficiently ductile the yield stress of the connected plates does not have to be exceeded to obtain full efficiency of the connection.

Figures 13, 14 and 15 are load Vs elongation curves for three typical series of tests representing the three ratios of l_2 to l_1 investigated. The importance of ductility is again illustrated in Figure 13. Use of the low ductility rutile electrode plus a low stress level in the connected plates severely penalized the connection.

The theoretical ultimate load for all specimens was determined by setting σ_E equal to the ultimate tensile strength of the weld material. From the load Vs elongation curves it appears that if σ_E was set equal to

the yield stress of the steel plates the resulting theoretical ultimate load would be within the elastic region of the curves. For design purposes this would be desirable. Therefore, the equations developed in this chapter could easily be used for design purposes and would predict the ultimate load with good accuracy.

As the yield stress for the steel used in this investigation was approximately one half the ultimate tensile stress of the electrodes used the yield stress of the steel would be a reasonable design stress, but for higher strength steels or lower strength electrodes this may or may not be true.

From the test data it appears that a minimum safety factor for static loading, so that stress in the weld material would be in the elastic range, is two. Thus, the maximum design stress should be one half the ultimate tensile stress of the weld material or the yield stress of the connected material, whichever is the smaller. Further protection against poor workmanship, variation in material strength, etc. should be provided by further reduction in the design stress.

CHAPTER V

COMPARISON OF PROPOSED THEORY WITH STANDARD AMERICAN PROCEDURE

To exemplify the accuracy of the theory proposed in the preceding chapters a comparison of the proposed theory to standard American theory will be presented in this chapter. Two general and widely used procedures for designing fillet welded joints are outlined in the following paragraphs.

For tensile loaded joints with concentric loading such as the I, II, and III series the usual procedure is to simply multiply the total throat area of the weldment by an allowable stress (see Figure 1c).[5]

$$P = (\Sigma a \ell)\sigma \qquad (64)$$

The loads predicted by such an analysis for all the I, II, and III series specimens along with the ratio of actual to predicted loads are listed in Table 10. For comparison the ratio of actual to theoretical loads as predicted by the theory presented in the preceding chapters is also listed. The ultimate tensile stress of the weld material was used in making the comparison.

As seen from Table 10 the ratios based on standard American practice are widely scattered. This is because orientation of the weldments to the direction of loading is not considered and proper load factors are not used to compensate for the orientation of the weldments. The predicted loads are unconservative by varying amounts except for the joints

with transverse welds only. This is true because the transverse welds are much stronger than the longitudinal welds when subjected to tensile loading along the longitudinal axis and not because of the accuracy of the method used for analysis. Therefore, joints designed by this method will have a varying safety factor with the magnitude depending upon the orientation of the weldments.

For joints subjected to eccentric loads the stresses are usually broken down into vectors along the x and y axis.[5] The stresses from the direct load are simply P/A as in the previous paragraph. The torsion formula ($\sigma = \frac{Mc}{J}$) is used to calculate stresses due to moment. The polar moment of inertia of the weld throat areas about an axis through and perpendicular to the center of rotation is used in the torsion formula. Again the center of gravity of the weld areas is assumed to be the center of rotation.

At points of maximum stress the vectors along the x and y axis are summed and then combined by taking the square root of the sum of the squares of the vectors. This combined stress is then multiplied by the available weld material throat area to determine the allowable load.

The loads predicted by such an analysis for all the IV, V, VI, and VII series specimens along with the ratio of actual to predicted loads are listed in Table 11. For comparison the ratio of actual to theoretical as predicted by the theory presented in the preceding chapters is also listed. The ultimate tensile stress of the weld material was used in making the comparison.

From Table 11 the ratios are observed to be widely scattered. The safety factor varies from one to greater than two. There does not appear

to be any definite trend to the magnitudes of the ratios except that they increase rapidly with increases in eccentricity.

This method is very conservative and would certainly be improved by taking into account the orientation of the welds to the direction of the applied forces and applying appropriate load factors as outlined in the previous chapters.

CHAPTER VI

CONCLUSIONS AND SUGGESTIONS FOR FURTHER STUDY

The following conclusions are drawn from this investigation and they must be limited to the conditions outlined in the preceding chapters.

1. Varying the ratio of areas of the transverse and longitudinal welds is a more significant parameter for investigation of a connection than the ratio of lengths or the ratio of throat depths of the transverse and longitudinal welds.

2. The stress level in the connected plates has a very significant effect upon the strength of a connection. As the stress level in the connected plates approaches or exceeds the yield stress of the connected plates, the higher the efficiency of the connection.

3. Ductility is of major importance in obtaining high efficiency for a connection. The weld metal must be ductile to allow redistribution of the stresses in the weld metal and this action is greatly aided if the connected plates are highly ductile also.

4. The basic interaction theory on fillet weld groups as proposed by the International Institute of Welding is correct if modified as in Chapter IV (see equation 60).

5. The design equations for "U" shaped weld groups as proposed by the International Institute of Welding do not produce consistent results and should be modified as shown in Chapter IV and outlined in Chapter VII.

The following are suggestions for additional study to verify the results and extend the scope of this investigation.

1. Obtain additional information on the effect of the ductility of the weld material and the connected plates on the efficiency of a connection.

2. Obtain additional information on the effect of varying ratios of weld areas on the effeciency of a connection.

3. Investigate connections with a range of ratios of torsional moment to direct load.

4. Investigate connections loaded with a direct load through the centroid of the weld group but at an angle to the longitudinal axis of the weld group.

CHAPTER VII

SUMMARY OF TENTATIVE RECOMMENDATIONS FOR DESIGN OF FILLET WELDED CONNECTIONS

The following recommendations for design are limited to connections that fall within the scope of this investigation.

1. Two longitudinal welds with concentric longitudinal loading:

$$\sigma_c = \frac{P}{0.8(\Sigma l_2 a_2)} \qquad (57)$$

2. One transverse weld with concentric longitudinal loading:

$$\sigma_c = \frac{P}{1.2(\Sigma l_1 a_1)} \qquad (58)$$

3. Combination of two longitudinal welds and one transverse weld with concentric longitudinal loading:

$$\sigma_c = \frac{P}{(1.2(\Sigma l_1 a_1) + 0.8(\Sigma l_2 a_2))} \qquad (59)$$

4. Two longitudinal welds with eccentric loading:

$$\sigma_c = \frac{P}{\Sigma l_2 a_2} \sqrt{0.35 \sin^2\theta + 1.56\left(\cos\theta + \frac{2e}{h + a_2}\right)^2} \qquad (61)$$

5. One transverse weld with eccentric loading:

$$\sigma_c = \frac{P}{\Sigma l_1 a_1} \sqrt{0.35\left(\frac{6e}{h} + \cos\theta\right)^2 + 1.56 \sin^2\theta} \qquad (62)$$

6. Combination of two longitudinal welds and one transverse weld with eccentric loading:

$$\sigma_c = \frac{(Eq.61)(Eq.62)}{Eq.61 + Eq.62} \qquad (63)$$

7. Combination of two longitudinal and two transverse welds with concentric longitudinal loading:*

$$\sigma_c = \frac{P}{\left(1.2(\Sigma l_1 a_1) + 0.8(\Sigma l_2 a_2)\right)} \qquad (64)$$

*These equations are not verified by test results but are logical extension of the results of this investigation.

8. Combination of two longitudinal and two transverse welds with eccentric loading:*

$$\sigma_c = \frac{P}{\Sigma l_1 a_1}\sqrt{0.35\left(\cos\theta + \frac{2e}{l_2+a_1}\right)^2 + 1.56\sin^2\theta}$$

$$+ \frac{P}{\Sigma l_2 a_2}\sqrt{0.35\left(\sin^2\theta + \frac{2e}{l_2+a_1}\right)^2 + 1.56\cos^2\theta} \qquad (65)$$

9. σ_c for use in the above equations should be one half the ultimate tensile stress of the weld metal or the yield stress of the connected plates, whichever is the smaller. This value of σ has a minimum safety factor of two against rupture. Further reduction in the design stress may be considered necessary for protection against poor workmanship, variation in material strength, etc.

*These equations are not verified by test results but are logical extensions of the results of this investigation.

APPENDIX A - Tables

Table 1. Actual Dimensions of Test Specimens

Code No.	t in.	h in.	l_1 in.	l_2 in.	a_1 in.	a_2 in.	$\Sigma l_1 a_1$ in.^{2}	$\Sigma l_2 a_2$ in.^{2}	e in.	θ deg.
IamR	1.287	1.774	1.774	3.07	0.132	0.171	0.468	2.092	0	0
IamR1	1.287	1.774	1.774		0.141		0.501		0	0
IamR2	1.287	1.774		3.10		0.179		2.215	0	0
IamR3	1.287	1.774		3.11		0.195		2.431	0	0
IbhA	1.287	1.777	1.777	3.13	0.147	0.124	0.524	1.545	0	0
IbhA1	1.287	1.777	1.777		0.148		0.539		0	0
IbhA2	1.287	1.777		3.13		0.141		1.769	0	0
IbhA3	1.287	1.777		3.13		0.181		2.266	0	0
IcsB	0.744	1.774	1.774	3.10	0.224	0.129	0.793	1.595	0	0
IcsB1	0.744	1.774	1.774		0.225		0.800		0	0
IcsB2	0.744	1.774		3.10		0.125		1.560	0	0
IcsB3	0.744	1.774		3.07		0.165		2.025	0	0
IIbmR	1.014	2.170	2.170	2.15	0.167	0.178	0.725	1.546	0	0
IIbmR	1.014	2.170	2.170	2.11	0.156	0.165	0.678	1.430	0	0
IIbmR	1.014	2.170	2.170	2.14	0.176	0.167	0.761	1.452	0	0
IIbmB	1.014	2.170	2.170	2.15	0.177	0.173	0.768	1.507	0	0
IIbmB	1.014	2.170	2.170	2.14	0.160	0.164	0.695	0.420	0	0
IIbmB	1.014	2.170	2.170	2.15	0.179	0.173	0.778	1.498	0	0
IIbmA	1.014	2.170	2.170	2.12	0.210	0.194	0.911	1.683	0	0
IIbmA	1.014	2.170	2.170	2.16	0.201	0.197	0.874	1.715	0	0
IIbmA	1.014	2.170	2.170	2.14	0.221	0.207	0.964	1.795	0	0
IIasA	0.744	2.170	2.170	2.14	0.115	0.208	0.500	1.778	0	0
IIasA1	0.744	2.170	2.170		0.128		0.554		0	0
IIasA2	0.744	2.170		2.13		0.199		1.698	0	0
IIasA3	0.744	2.170		2.11		0.268		2.262	0	0

Table 1. Actual Dimensions of Test Specimens (Continued)

Code No.	t in.	h in.	l_1 in.	l_2 in.	a_1 in.	a_2 in.	$\Sigma l_1 a_1$ in.^{2}	$\Sigma l_2 a_2$ in.^{2}	e in.	ϕ deg.
IIbmB	1.015	2.170	2.170	2.15	0.178	0.168	0.771	1.448	0	0
IIbmB1	1.015	2.170	2.170		0.202		0.877		0	0
IIbmB2	1.015	2.170		2.15		0.174		1.497	0	0
IIbmB3	1.015	2.170		2.16		0.279		2.402	0	0
IIchR	1.287	2.167	2.167	2.11	0.297	0.147	1.288	1.241	0	0
IIchR1	1.287	2.167	2.167		0.314		1.364		0	0
IIchR2	1.287	2.167		2.11		0.158		1.331	0	0
IIchR3	1.287	2.167		2.13		0.311		2.639	0	0
IIIahB	1.014	3.152	3.152	1.57	0.157	0.258	0.992	1.621	0	0
IIIahB1	1.014	3.152	3.152		0.169		1.069		0	0
IIIahB2	1.014	3.152		1.57		0.248		1.564	0	0
IIIahB3	1.014	3.152		1.57		0.354		2.227	0	0
IIIbsR	0.615	3.152	3.152	1.58	0.183	0.195	1.154	1.225	0	0
IIIbsR1	0.615	3.152	3.152		0.201		1.263		0	0
IIIbsR2	0.615	3.152		1.57		0.207		1.304	0	0
IIIbsR3	0.615	3.152		1.57		0.333		2.097	0	0
IIIcmA	0.746	3.153	3.153	1.57	0.318	0.150	2.005	0.943	0	0
IIIcmA1	0.746	3.153	3.153		0.332		2.089		0	0
IIIcmA2	0.746	3.153		1.58		0.145		0.915	0	0
IIIcmA3	0.746	3.153		1.57		0.343		2.158	0	0
IVbmB	1.014	2.162	2.162	2.16	0.175	0.164	0.759	1.417	7	90
IVbmB1	1.014	2.162	2.162		0.196		0.846		7	90
IVbmB2	1.014	2.162		2.17		0.184		1.602	7	90

Table 1. Actual Dimensions of Test Specimens (Continued)

Code No.	t in.	h in.	l_1 in.	l_2 in.	a_1 in.	a_2 in.	$\Sigma l_1 a_1$ in.^{2}	$\Sigma l_2 a_2$ in.^{2}	e in.	ϕ deg.
VbsB	0.745	3.152	3.152	1.65	0.165	0.159	1.039	1.048	7	90
VbsB1	0.745	3.152	3.152		0.174		1.096		7	90
VbsB2	0.745	3.152		1.61		0.161		1.037	7	90
VIbmB	1.014	2.162	2.162	2.18	0.170	0.162	0.734	1.409	8.5	45
VIbmB1	1.014	2.162	2.162		0.165		0.712		8.5	45
VIbmB2	1.014	2.162		2.17		0.166		1.445	8.5	45
VIIbsB	0.745	3.152	3.152	1.64	0.164	0.166	1.031	1.087	8.5	45
VIIbsB1	0.745	3.152	3.152		0.163		1.024		8.5	45
VIIbsB2	0.745	3.152		1.63		0.166		1.086	8.5	45

Table 2. Tensile Coupon Results for Parent Steel

Series Code No.	t in.	σ_y ksi	ϵ_{st} in./in.	σ_{ult} ksi	ϵ_{ult} in./in.	Elongation %	Reduction in Area %
IamR	1.287	33.1	0.010	65.1	0.317	31.7	64.0
IbhA	1.287	33.1	0.010	65.1	0.317	31.7	64.0
IcsB	0.745	32.9	0.011	63.6	0.281	28.1	54.2
IIasA	0.745	31.9	0.011	63.5	0.288	28.8	57.2
IIbmB	1.014	32.9	0.011	64.4	0.297	29.7	52.4
IIchR	1.287	32.9	0.014	64.7	0.316	31.6	63.0
IIIahB	1.014	33.6	0.011	65.8	0.302	30.2	48.1
IIIbsR	0.615	35.5	0.012	65.3	0.276	27.6	50.6
IIIcmA	0.745	32.0	0.013	62.1	0.288	28.8	56.1
IVbmB	1.014	33.2	0.011	65.0	0.300	30.0	51.5
VbsB	0.745	32.0	0.012	62.8	0.288	28.8	56.5
VIbmB	1.014	33.2	0.011	65.0	0.300	30.0	51.5
VIIbsB	0.745	32.0	0.012	62.8	0.288	28.8	56.5

Table 3. Tensile Coupon Results for Deposited Weld Material

Electrode	Type	ksi	in./in.	ksi	in./in.	Elongation %	Reduction in Area %
E-7014	R	59.5	0.224	68.5	0.223	22.3	41.3
E-7018	B	65.5	0.247	79.1	0.130	13.0	22.5
E-6027	A	53.8	0.204	65.9	0.315	31.5	60.7

Table 4. Test Results and Analysis for Longitudinal Welds with Concentric Loading

Code No.	P (actual) Kips	P_{IIW} Formula Number 3 σ =71ksi Kips	P_{IIW} Formula Number 3 $\sigma = \sigma_\omega$ Kips	P/P_{IIW} $\sigma = \sigma_\omega$	$\frac{P/A}{\sigma_\omega}$ = Load Factor
IamR2	119	118	114	1.05	0.79
3	120	129	125	0.96	0.72
IbhA2	115	94	88	1.31	0.98
3	129	121	112	1.15	0.87
IcsB2	112	83	93	1.21	0.91
3	139	108	120	1.15	0.87
IIasA2	89	90	84	1.06	0.79
3	118	120	112	1.05	0.79
IIbmB2	93	80	90	1.05	0.78
3	150	128	142	1.05	0.79
IIchR2	73	71	68	1.07	0.80
3	134	140	136	0.99	0.74
IIIahB2	106	83	93	1.14	0.85
3	138	118	132	1.04	0.78
IIIbsR2	66	69	67	0.98	0.73
3	106	111	108	0.98	0.74
IIIcmA2	68	49	45	1.50	1.13
3	121	115	106	1.14	0.85

Table 5. Test Results and Analysis for Transverse Welds with Concentric Loading

Code No.	P (actual) Kips	P_{IIW} Formula Number 6 σ =71ksi Kips	P_{IIW} Formula Number 6 $\sigma = \sigma_\omega$ Kips	P/P_{IIW} $\sigma = \sigma_\omega$	$\frac{P/A}{\sigma_\omega}$ = Load Factor
IamR1	38	30	29	1.30	1.11
IbhA1	54	33	30	1.77	1.50
IcsB1	65	48	54	1.21	1.03
IIasA1	51	33	31	1.64	1.40
IIbmB1	82	53	59	1.38	1.18
IIchR1	100	82	79	1.26	1.07
IIIahB1	122	65	72	1.70	1.44
IIIbsR1	104	76	74	1.41	1.20
IIIcmA1	159	126	117	1.36	1.16

Table 6. Test Results and Analysis for a Combination of Two Longitudinal Welds and One Transverse Weld with Concentric Loading

Code No.	P (actual) Kips	P_{IIW} Formula #7,8&9 σ = 71ksi Kips	P_{IIW} Formula #7,8&9 $\sigma = \sigma_\omega$ Kips	P/P_{IIW}	$P_{Revised}$ Formula #59 $\sigma = \sigma_\omega$ Kips	$P/P_{Revised}$	Stress Level in Steel σ_s/σ_y
IIbmR	136	98	94	1.45	145	0.94	0.93
IIbmR	139	90	87	1.61	134	1.04	1.00
IIbmR	135	93	90	1.51	142	0.95	0.93
IIbmB	167	96	107	1.56	168	0.99	1.14
IIbmB	167	90	100	1.67	156	1.07	1.14
IIbmB	163	96	107	1.53	168	0.97	1.11
IIbmA	165	108	100	1.64	161	1.03	1.13
IIbmA	174	109	101	1.72	160	1.08	1.19
IIbmA	170	115	106	1.60	171	1.00	1.16
IamR	125	110	108	1.16	152	0.82	0.82
IbhA	148	82	76	1.94	123	1.20	1.00
IcsB	160	85	95	1.69	176	0.91	Ruptured Steel
IIasA	136	105	97	1.40	133	1.02	1.31
IIbmB	155	92	103	1.50	165	0.94	0.96
IIchR	161	92	88	1.82	173	0.93	0.87
IIIahB	213	90	99	2.17	197	1.08	1.00
IIIbsR	160	92	89	1.81	162	0.99	1.16
IIIcmA	200	138	158	1.58	208	0.97	1.33

Table 7. Test Results and Analysis for Two Longitudinal Welds with Eccentric Loading

Code No.	P (actual) Kips	P_{IIW} Formula No. 14 σ = 71ksi Kips	P_{IIW} Formula No. 14 $\sigma = \sigma_\omega$ Kips	P/P_{IIW}	$P_{revised}$ Formula No. 61 $\sigma = \sigma_\omega$ Kips	$P/P_{revised}$
IVbmB2	22.5	14.1	15.7	1.44	17.0	1.32
VbsB2	19.5	12.8	14.2	1.37	15.5	1.26
VIbmB2	21.0	10.4	11.6	1.80	14.6	1.40
VIIbsB2	15.6	11.1	12.3	1.27	14.0	1.12

Table 8. Test Results and Analysis for One Transverse Weld with Eccentric Loading

Code No.	P (actual)	P_{IIW} Formula No. 30		P/P_{IIW}	$P_{revised}$ Formula No. 62	$P/P_{revised}$
		σ = 71ksi	$\sigma = \sigma_\omega$		$\sigma = \sigma_\omega$	
	Kips	Kips	Kips		Kips	
IVbmBl	7.1	2.61	2.90	2.46	5.85	1.21
VbsBl	13.7	4.93	5.48	2.51	11.00	1.24
VIbmBl	4.0	1.72	1.92	2.08	3.92	1.02
VIIbsBl	9.6	3.79	4.22	2.27	8.10	1.19

Table 9. Test Results and Analysis for a Combination of Two Longitudinal Welds and One Transverse Weld with Eccentric Loading

Code No.	P (actual)	P_{IIW} Formula No. 55		P/P_{IIW}	$P_{revised}$ Formula No. 63	$P/P_{revised}$
		σ = 71ksi	$\sigma = \sigma_\omega$		$\sigma = \sigma_\omega$	
	Kips	Kips	Kips		Kips	
IVbmB	27.2	9.7	10.8	2.50	20.8	1.30
VbsB	30.8	12.0	13.4	2.32	26.1	1.18
VIbmB	26.7	7.9	8.8	3.04	17.5	1.52
VIIbsB	28.4	9.4	10.5	2.70	22.2	1.28

Table 10. Comparison of Theoretical Loads for Concentrically Loaded Joints Using a Standard Method and the Proposed Method

Code No.	P (actual) Kips	P Standard American Method Kips	$P_{revised}$ Kips	R Standard American Method	$R_{revised}$
IamR	125	175	152	0.72	0.82
IamR1	38	34	41	1.12	0.93
IamR2	119	152	121	0.79	0.99
IamR3	120	167	133	0.72	0.91
IbhA	148	137	123	1.08	1.20
IbhA1	54	35	43	1.50	1.25
IbhA2	115	117	93	0.98	1.24
IbhA3	129	149	120	0.87	1.07
IcsB	160	190	176	Rupture of Steel	
IcsB1	65	63	75	1.03	0.87
IcsB2	112	123	99	0.91	1.13
IcsB3	139	160	128	0.87	1.08
IIbmR	136	160	145	0.87	0.94
IIbmR	139	146	134	0.95	1.04
IIbmR	135	153	142	0.88	0.95
IIbmB	167	181	168	0.92	0.99
IIbmB	167	169	156	0.99	1.07
IIbmB	163	181	168	0.90	0.97
IIbmA	165	172	161	0.96	1.03
IIbmA	174	172	160	1.01	1.08
IIbmA	170	183	171	0.93	1.00
IIasA	136	150	133	0.90	1.02
IIasA1	51	36	44	1.40	1.15
IIasA2	89	112	89	0.79	1.00
IIasA3	118	148	119	0.79	1.00
IIbmB	155	175	165	0.88	0.94
IIbmB1	82	69	83	1.18	1.00
IIbmB2	93	118	94	0.78	1.00
IIbmB3	150	190	152	0.79	1.00
IIchR	161	173	173	0.93	0.93
IIchR1	100	94	112	1.07	0.90
IIchR2	73	92	73	0.80	1.00
IIchR3	134	182	144	0.74	0.94

Table 10. Comparison of Theoretical Loads for Concentrically Loaded Joints Using a Standard Method and the Proposed Method (Continued)

Code No.	P (actual) Kips	P Standard American Method Kips	$P_{revised}$ Kips	R Standard American Method	$R_{revised}$
IIIahB	214	207	197	1.03	1.08
IIIahB1	122	84	102	1.44	1.19
IIIahB2	106	124	99	0.85	1.07
IIIahB3	138	176	141	0.78	0.98
IIIbsR	160	163	162	0.98	0.99
IIIbsR1	104	87	104	1.20	1.00
IIIbsR2	66	89	71	0.73	0.93
IIIbsR3	106	144	115	0.74	0.93
IIIcmA	200	194	208	1.04	0.97
IIIcmA1	159	138	164	1.16	0.97
IIIcmA2	68	60	49	1.13	1.37
IIIcmA3	121	142	114	0.85	1.06

Table 11. Comparison of Theoretical Loads for Eccentrically Loaded Joints Using a Standard Method and the Proposed Method

Code No.	P (actual) Kips	P Standard American Method Kips	$P_{revised}$ Kips	R Standard American Method	$R_{revised}$
IVbmB	27.2	24.8	20.8	1.11	1.30
IVbmB1	7.1	3.45	5.85	2.06	1.21
IVbmB2	22.5	16.5	17.0	1.36	1.31
VbsB	30.8	26.7	26.1	1.15	1.18
VbsB1	13.7	6.52	11.0	2.10	1.24
VbsB2	19.5	16.1	15.5	1.21	1.26
VIbmB	26.7	14.5	17.5	1.84	1.52
VIbmB1	4.0	2.39	3.92	1.67	1.02
VIbmB2	21.0	12.2	14.6	1.72	1.40

Table 11. Comparison of Theoretical Loads for Eccentrically Loaded Joints Using a Standard Method and the Proposed Method (Continued)

Code No.	P (actual) Kips	P Standard American Method Kips	$P_{revised}$ Kips	R Standard American Method	$R_{revised}$
VIIbsB	28.4	17.3	22.2	1.64	1.28
VIIbsB1	9.6	5.04	8.1	1.91	1.19
VIIbsB2	15.6	12.9	14.0	1.21	1.12

APPENDIX B - Figures

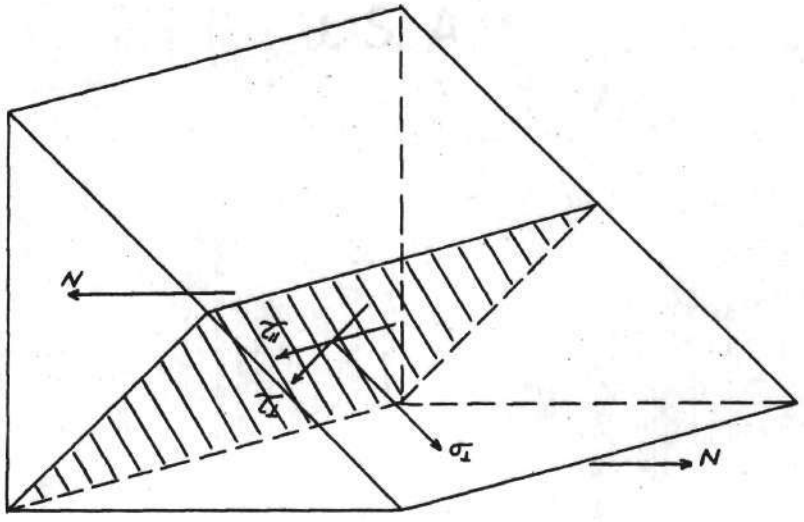

Fig. 1a. Direction and location of Stresses on the Weldment.

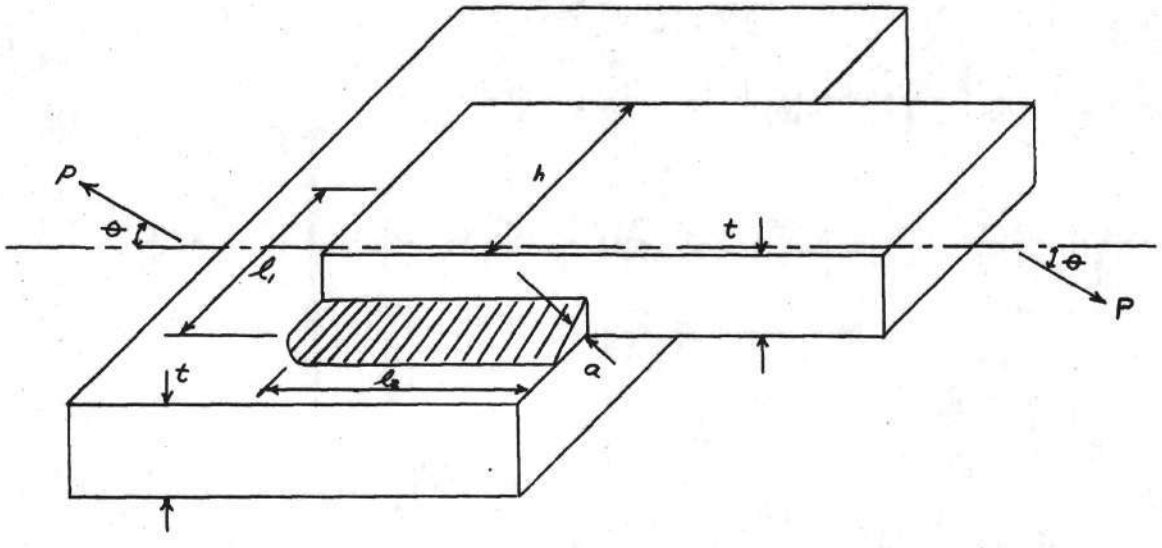

Fig. 1b. General Dimensions of Test Specimen.

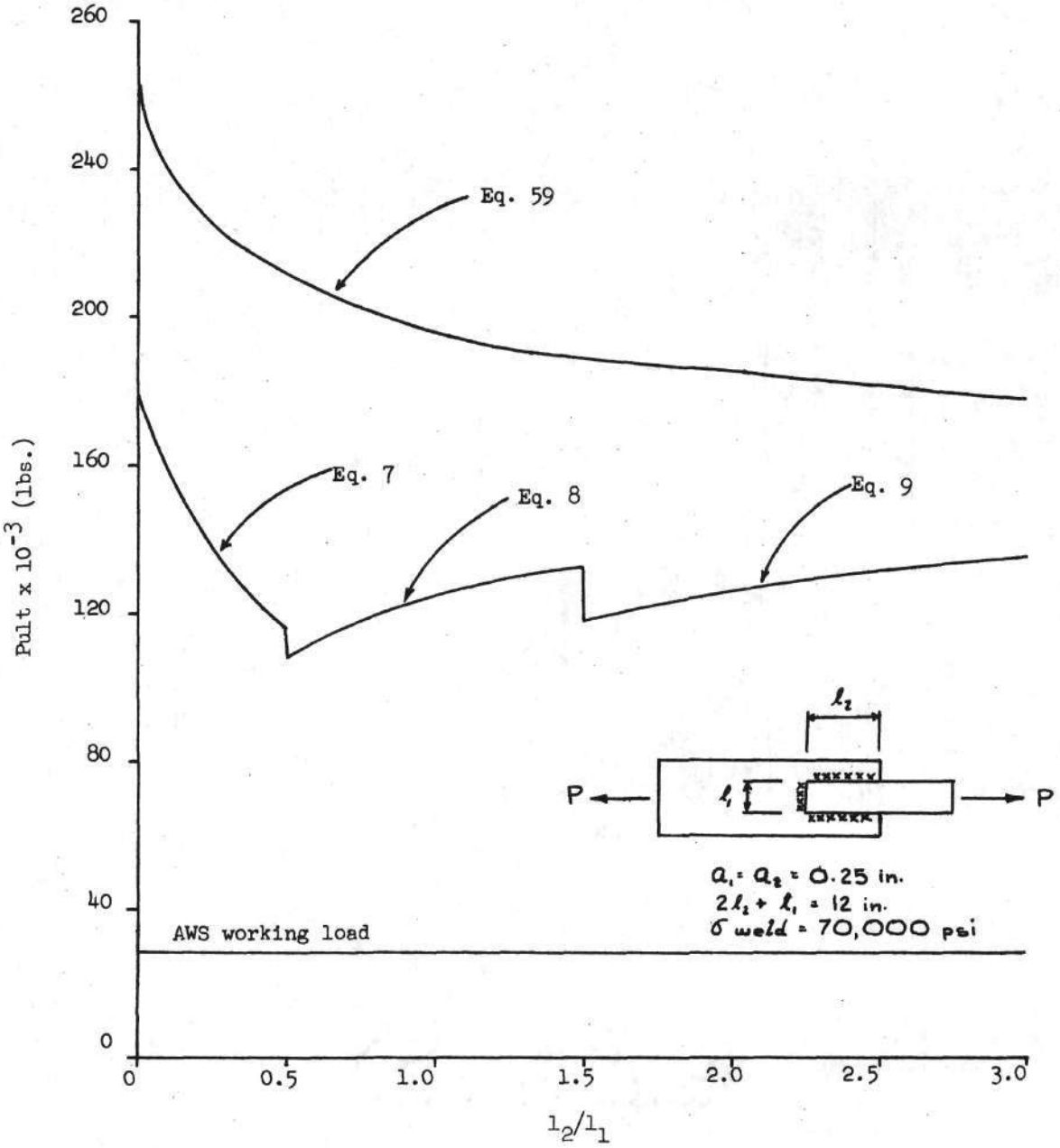

Fig. 1c. Comparison of Theoretical Ultimate Loads.

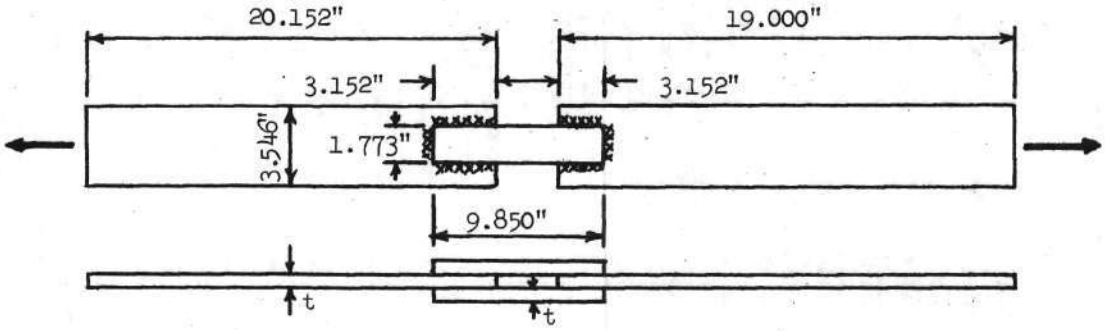

Class I

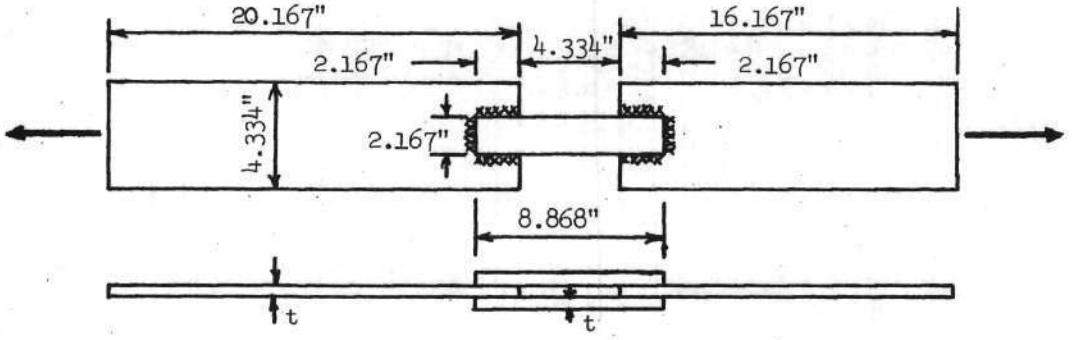

Class II

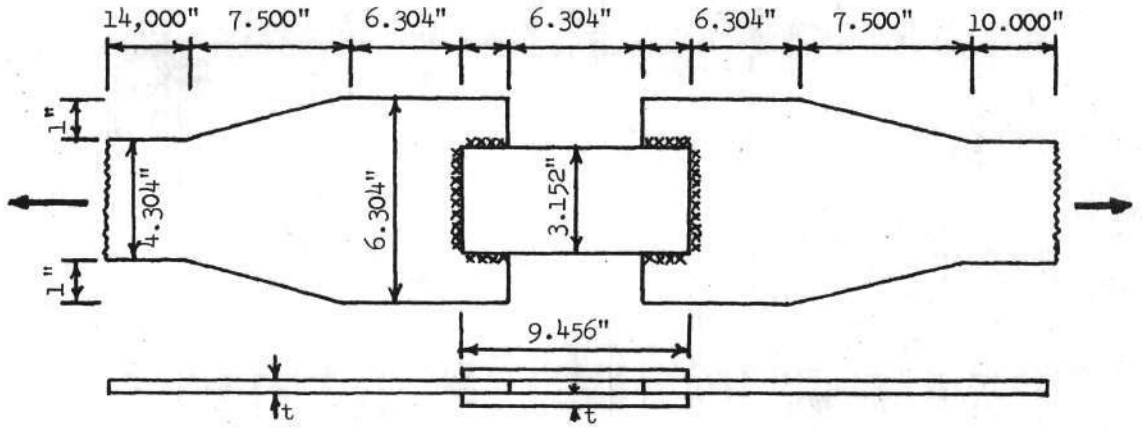

Class III

Fig. 2. Test Specimens Loaded in Tension

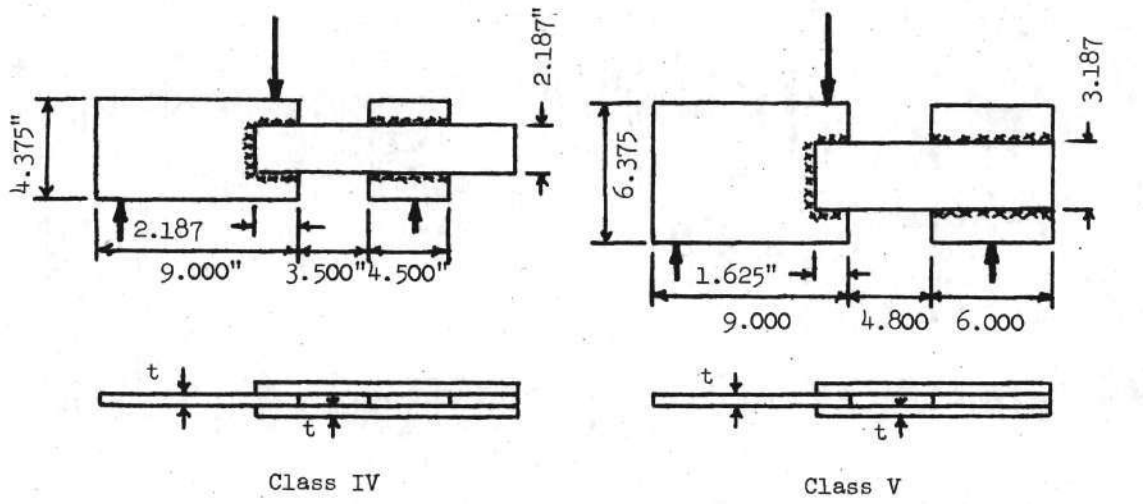

Fig. 3. Test Specimens Loaded in Shear and Torsional Moment

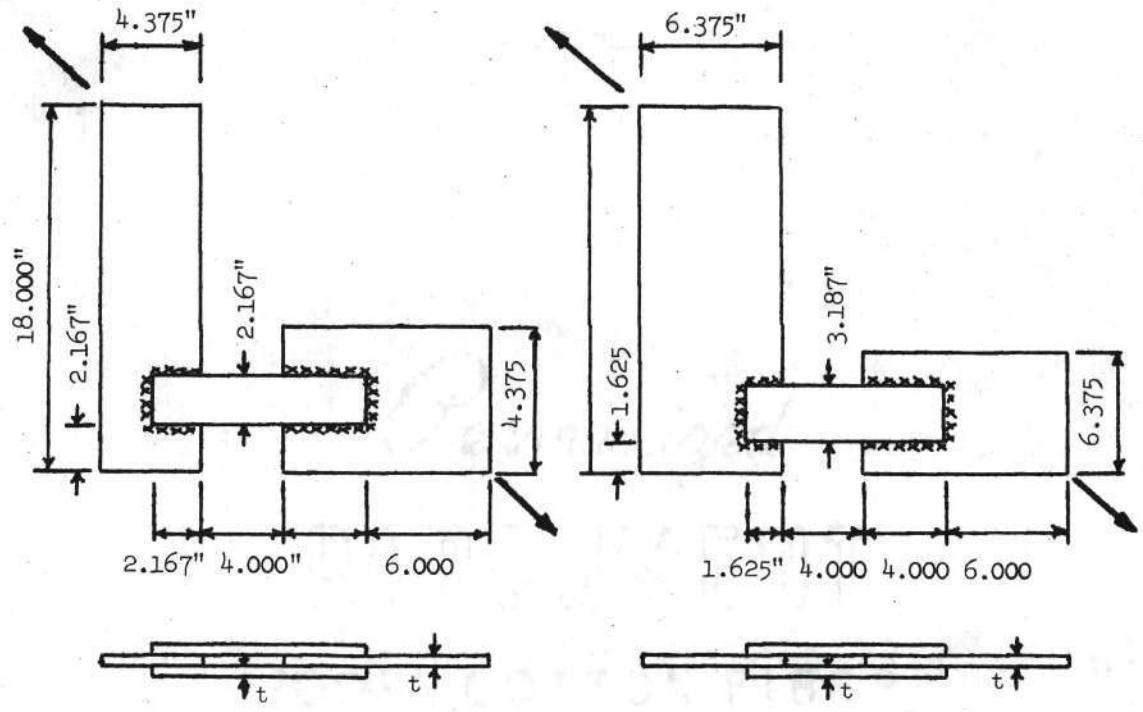

Fig. 4. Test Specimens Loaded in Shear, Torsional Moment and Tension

1-1/4 in Steel Plate

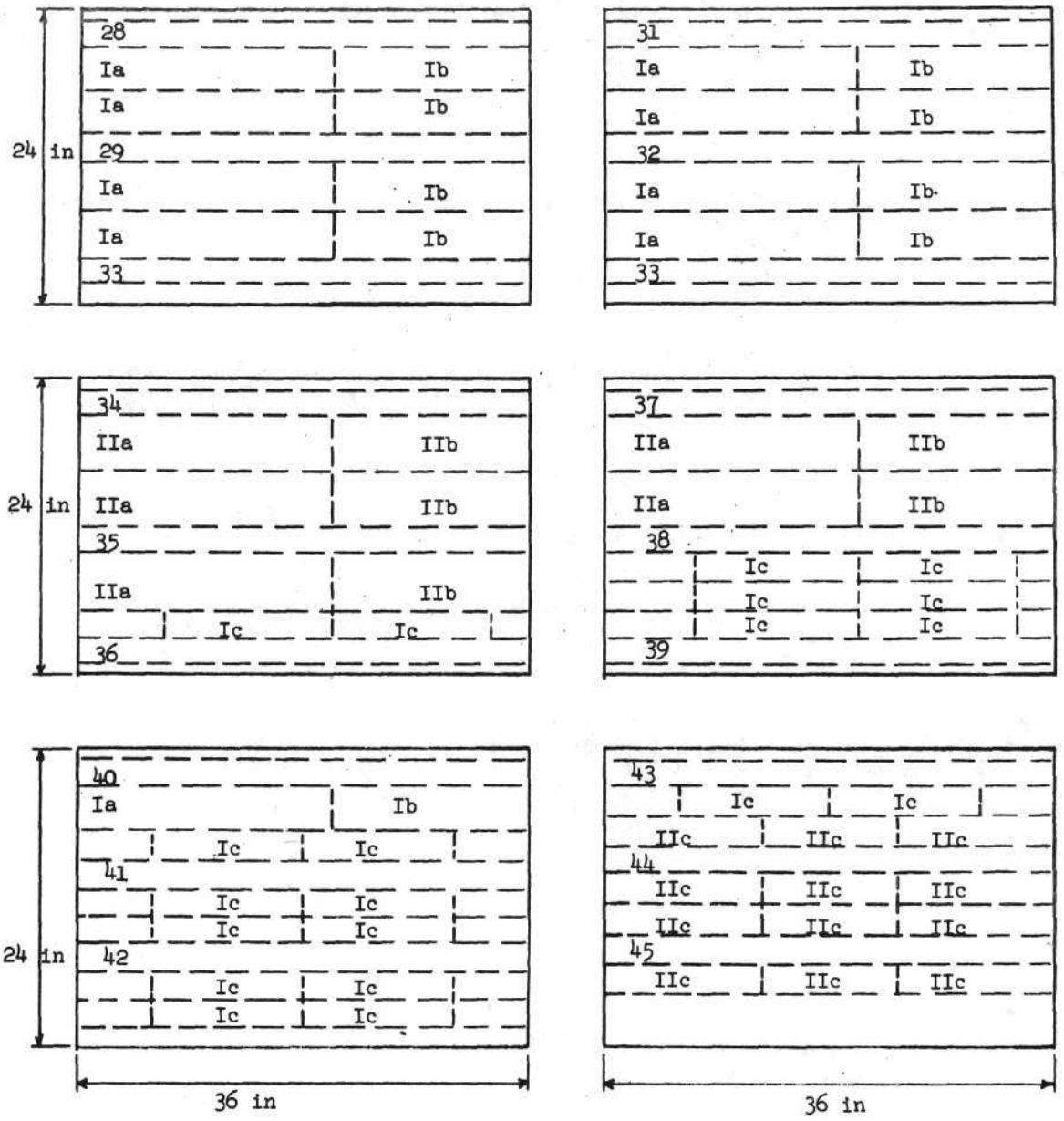

Fig. 5. Typical Coupon Layout on Steel Plate

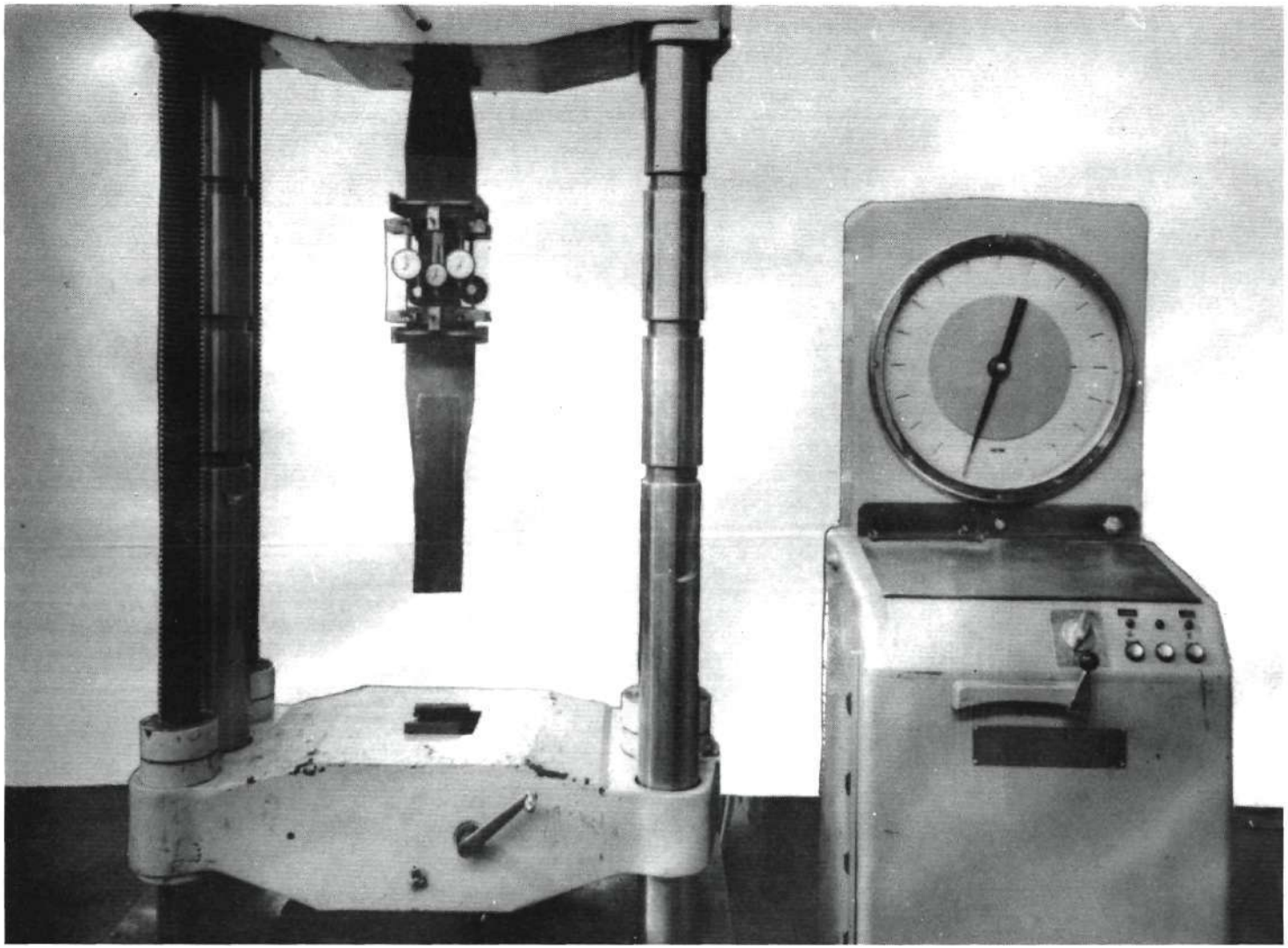

Figure 6. Typical Test Arrangement.

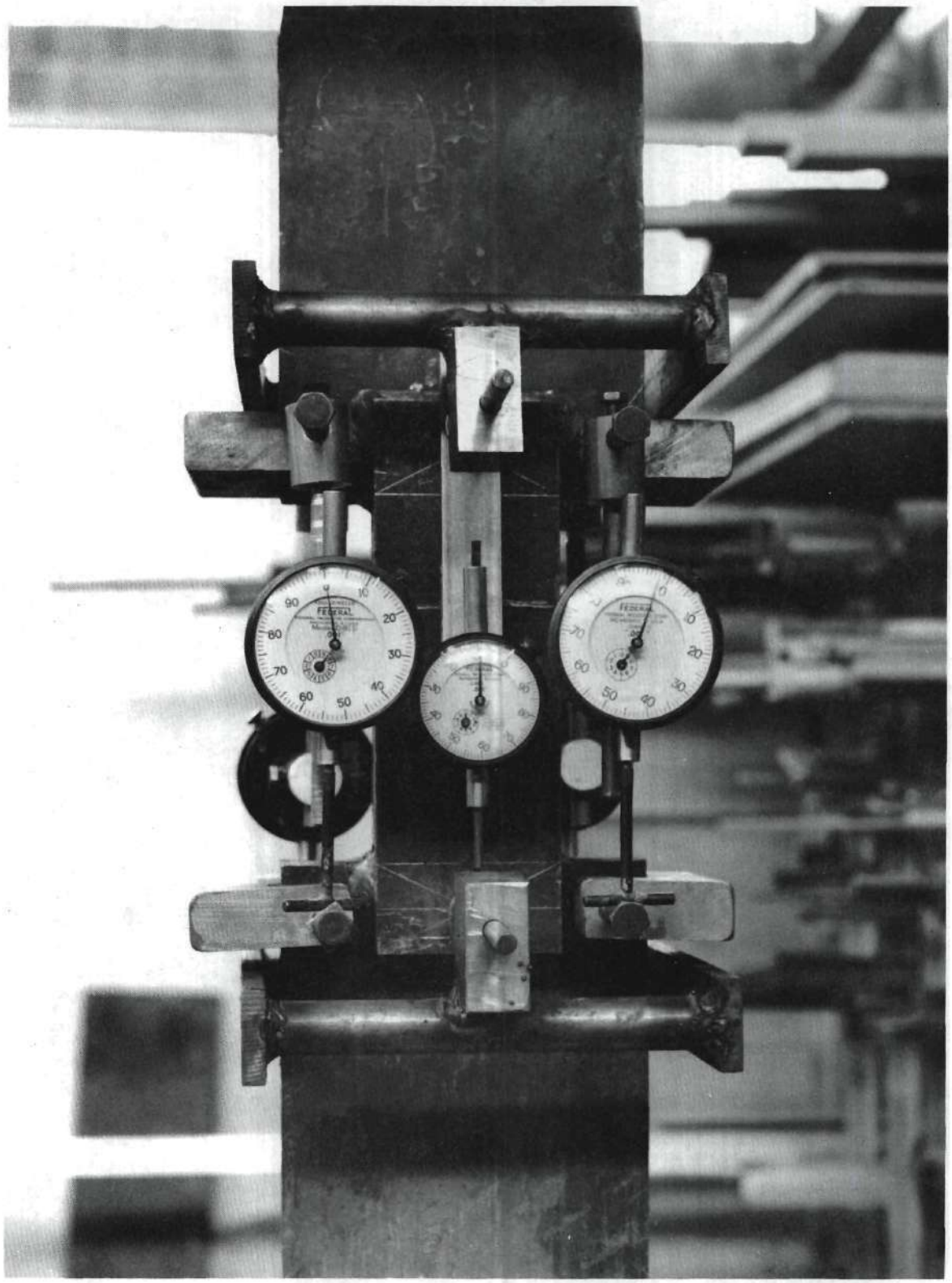

Figure 7. Test Specimen and Instrumentation.

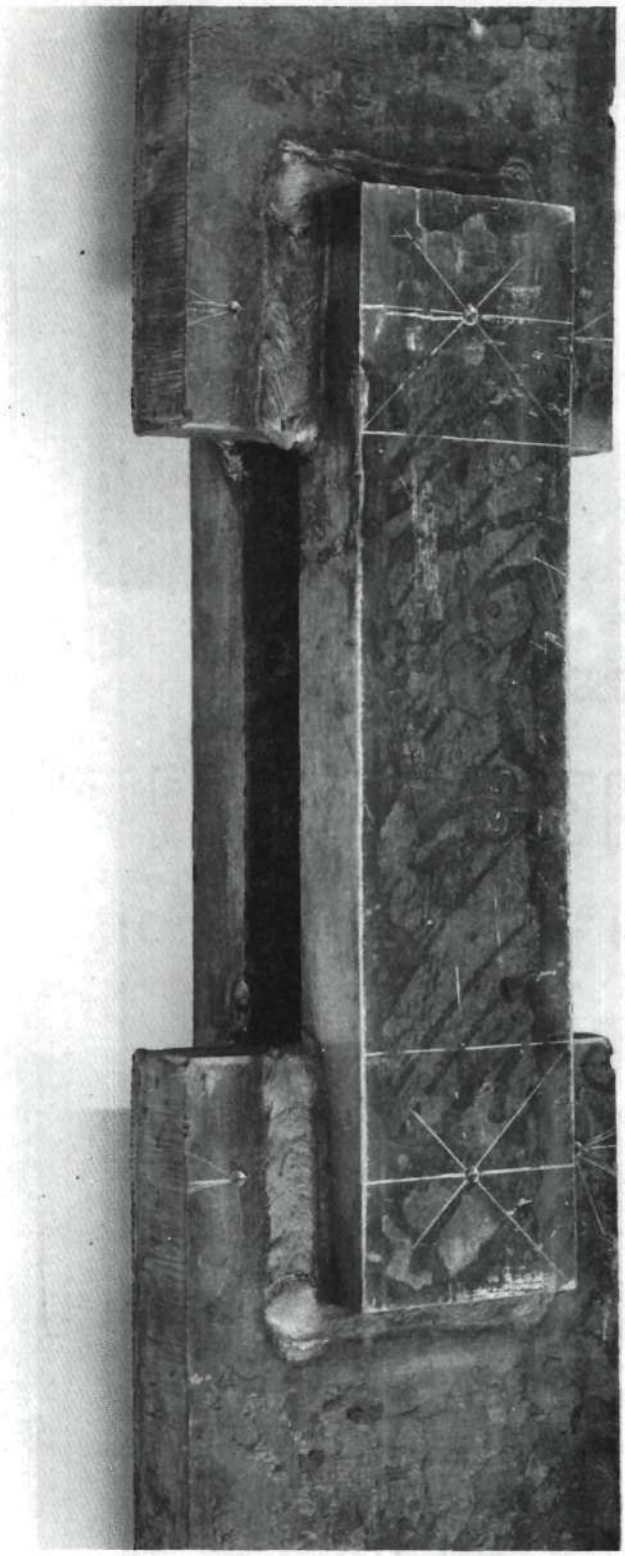

Figure 8. Test Specimen Before Loading.

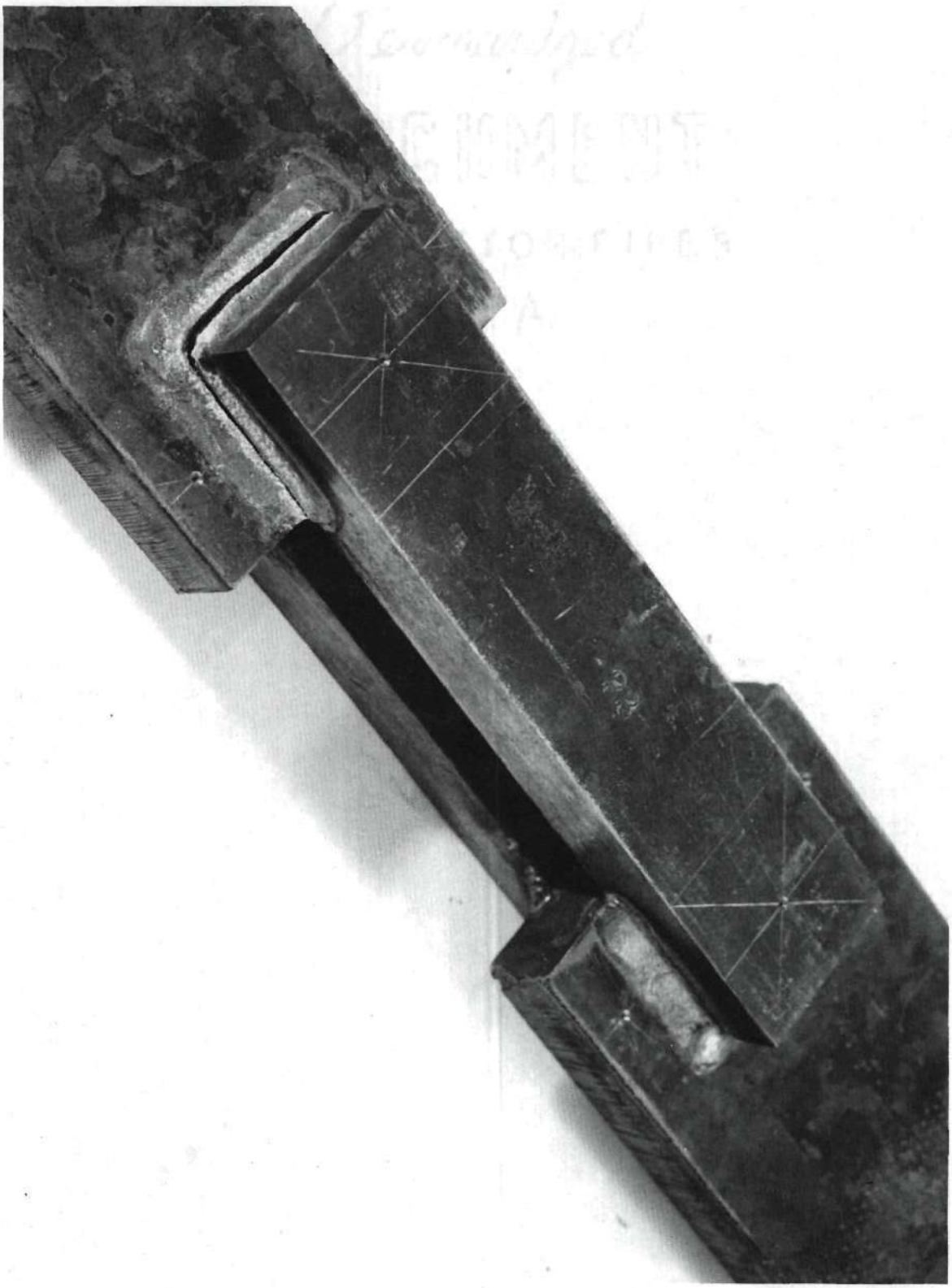

Figure 9. Test Specimen After Loading.

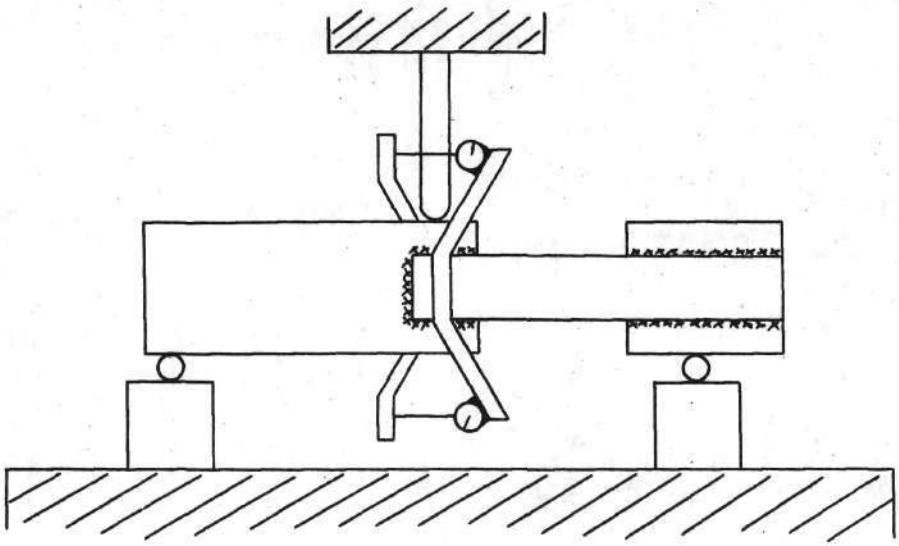

Fig. 10. Instrumentation of Specimens Loaded in Shear and Torsional Moment.

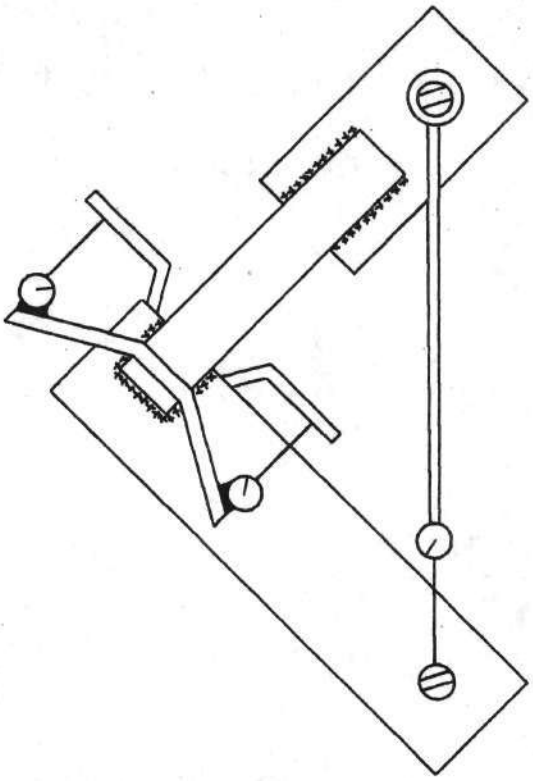

Fig. 11. Instrumentation of Specimens Loaded in Torsional Moment Shear and Tension.

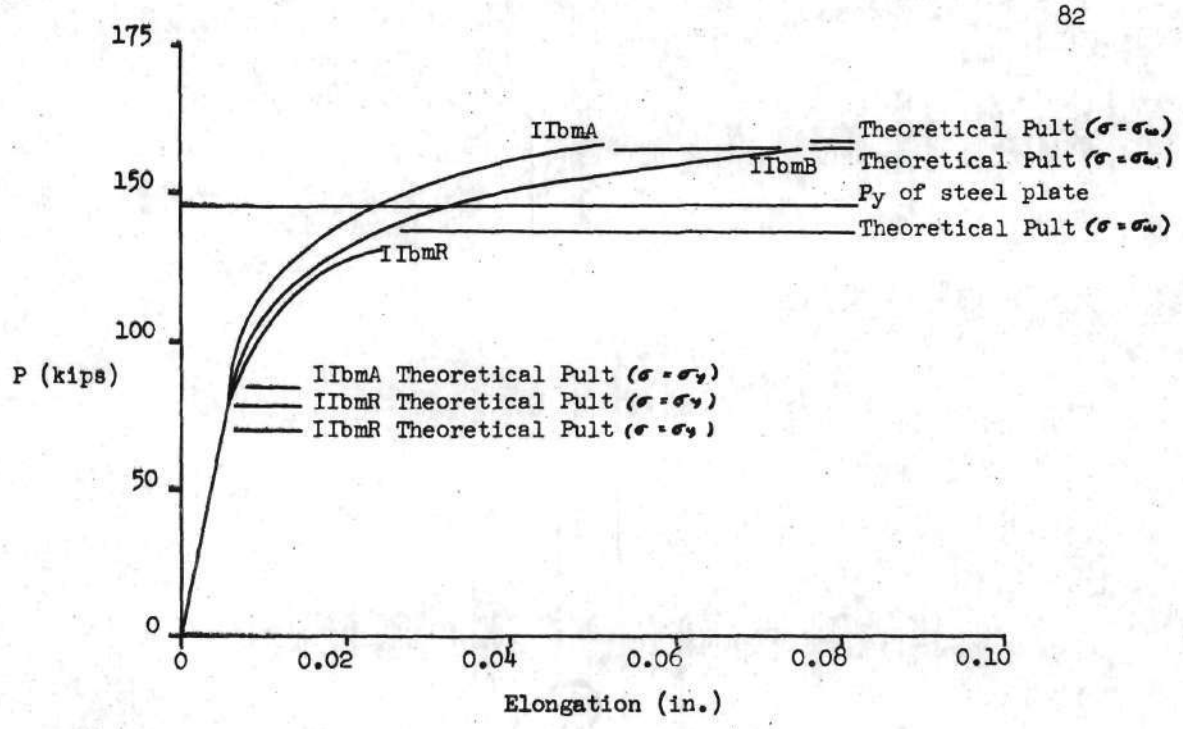

Fig. 12. Load vs Average Elongation of Weld Material Curves for Specimens IIbmA, IIbmB and IIbmR.

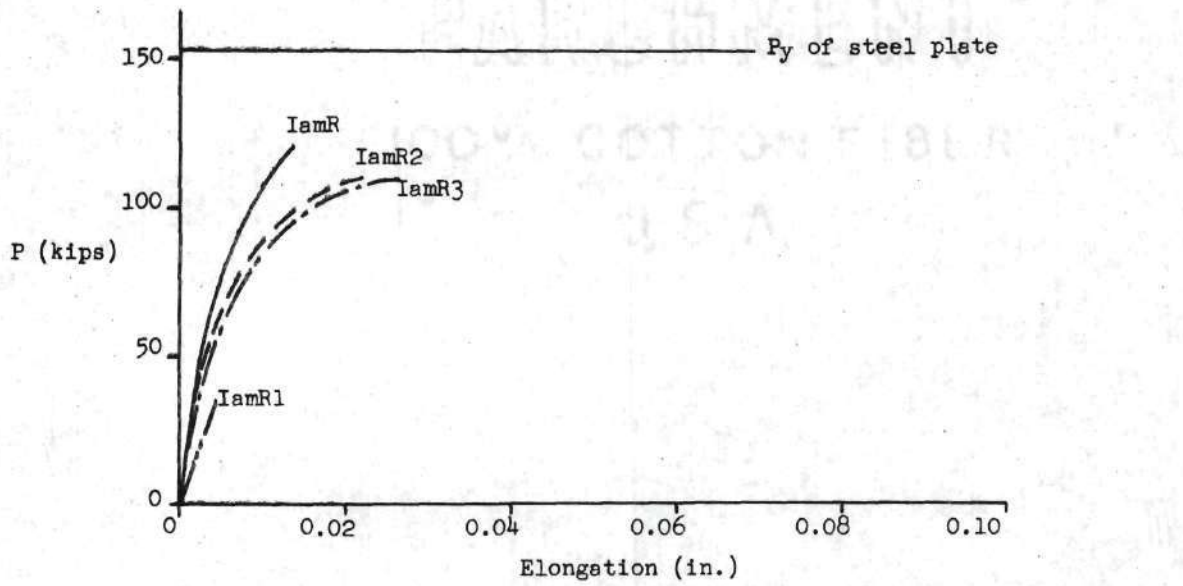

Fig. 13. Load vs Average Elongation of Weld Material Curves for Specimens IamR, 1, 2 and 3.

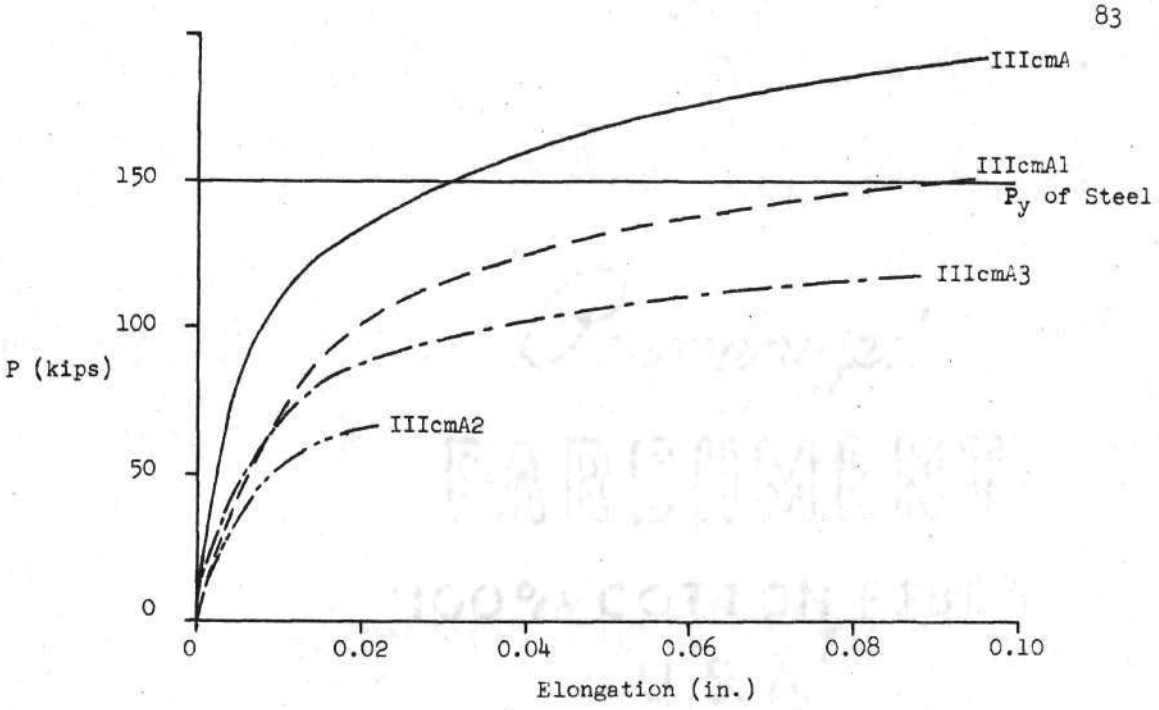

Fig. 15. Load vs Average Elongation of Weld Material Curves for Specimens IIIcmA, 1, 2 and 3.

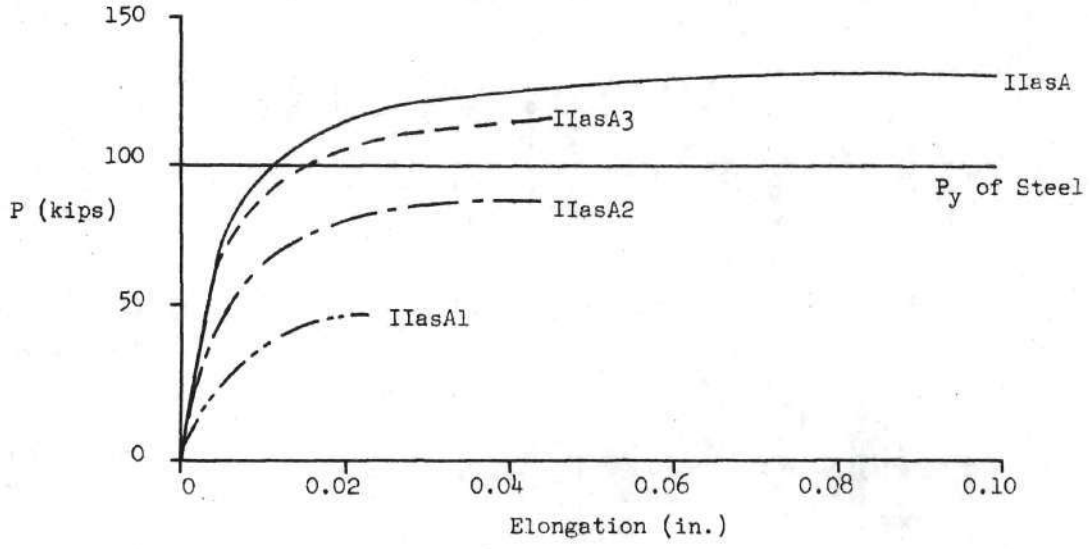

Fig. 14. Load vs Average Elongation of Weld Material Curves for Specimens IIasA, 1, 2 and 3.

BIBLIOGRAPHY

1. Calculation Formulas for Welded Connections Submitted to Static Loads, International Institute of Welding, Doc. XV-107-60, 1960.

2. ASTM Standards, Part I, Ferrous Metals Specifications, American Society for Testing Materials, page 551, 1961.

3. ASTM Standards, Part 3, Metals Test Methods (Except Chemical Analysis), American Society for Testing Materials, page 165, 1961.

4. Welding Handbook, Section One, American Welding Society, page 9.6, 1957.

5. Design of Steel Structures, Bresler, Boris, and Lin, T. Y., New York: John Wiley and Sons, Inc., 1960, page 200.